5-2019

Acquisition of Hockey Goalies Kinematic Data Using Motion Capture Systems

Tzu-Ting Hsu

Acquisition of Hockey Goalies Kinematic Data Using Motion Capture Systems

By Tzu-Ting (Tiffany) Hsu, Master of Science in Mechanical Engineering

Thesis Advisor: Kathleen Lamkin-Kennard, Ph.D. Rochester Institute of Technology

Kate Gleason College of Engineering

Department of Mechanical Engineering

Rochester Institute of Technology

Rochester, NY

May,2019

Acquisition of Hockey Goalies Kinematic Data Using Motion Capture Systems

By Tzu-Ting (Tiffany) Hsu, Master of Science, Rochester Institute of Technology

Thesis Advisor: Kathleen Lamkin-Kennard, Ph.D. Rochester Institute of Technology

Kate Gleason College of Engineering

Department of Mechanical Engineering

Rochester Institute of Technology

Rochester, NY

May,2019

Approved by:

_____

Dr. Kathleen Lamkin-Kennard
Thesis Advisor, Department of Mechanical Engineering

_____

Dr. Mario Gomes
Committee Member, Department of Mechanical Engineering

_____

Dr. William Brewer
Committee Member, Department of Exercise Science

_____

Dr. Ehsan Rashedi
Committee Member, Department of Industrial and Systems Engineering

_____

Dr. Stephen Boedo
Department Representative, Department of Mechanical Engineering

Acknowledgements

The topic of this thesis is very personal to me. Thank you to my thesis advisor, Dr. Kathleen Lamkin-Kennard, who helps me make my vision come true. I never envisioned I would be able to get this far with the concept I had in my mind when I first brought the idea of this thesis to her.

Special thanks to Dr. Ehsan Rashedi for letting me use his lab equipment and sharing his knowledge on biomechanical research with me. Thanks to Dr. William Brewer for providing help and additional point of view from the anatomy stand point. Thank you to Dr. Mario Gomes for providing insights on instrumental and random uncertainties.

Big thank you to Masoud Abdollahi and Maya Luster for helping me with data collection. Thanks to Jamie Marsden for performing range of motion tests. Last but not least, thank you to all the staff at Ritter Arena for allowing me to use the facility for data collection. Without you all, this thesis would not be completed.

Abstract

Hockey goalies all over the world have adopted the butterfly style of goaltending due to the fast pace of the game. However, the style of play has brought the potential for injuries to goalies. In this study, a motion capture system was used to analyze the butterfly motion performed by a human subject to quantify the kinematics and kinetics associated with the motion. Further analysis was done with the motion capture data to obtain the joint angles of the hip and the knee joints and the forces in the joints associated with the butterfly motions. Through the experiments, the kinematics and joint angles were obtained. With the data obtained, the kinetics, joint reaction forces and moments associated with the butterfly motions were calculated using inverse dynamics modeling. Results from the thesis showed abnormally large joint reaction forces and moments during butterfly motions, in comparison to normal walking motions, and could increase the potential for knee injuries.

Table of Contents

List of Figures

List of Figures

Nomenclature

AAOS = American Academy of Orthopaedic Surgeons

ACL = Anterior Cruciate Ligament

AMTI = Advanced Mechanical Technology Inc.

AP = Access Point

ASI = Anterior Superior Iliac

CMC = Coefficient of Multiple Correlation

COM = Center of Mass

COP = Center of Pressure

DKV = Dynamic Knee Valgus

EMG = Electromyography

FAI = Femoroacetabular Impingement

IMU = Inertial Measurement Unit

JRF = Joint Reaction Force

JRM = Joint Reaction Moment

LCL = Lateral Collateral Ligament

MCL = Medial Collateral Ligament

NHL = National Hockey League

PCL = Posterior Cruciate Ligament

PFP = Patellofemoral Pain

ROM = Range of Motion

V3D = Visual 3D

V3D = Visual3D

1.0 Problem Introduction

Equipment is essential for the prevention of injuries. As equipment technology has improved, the speed of hockey games has gotten faster. The faster game has brought a dramatic amount of change to goaltending strategies and the goalie's job has become significantly harder. To adapt to these changes, the butterfly style of goaltending was born. The butterfly style gives goalies better coverage due to the wide-spread movement of the legs, but it also increases the possibility of injuries to the knees, hips, and joints due to the awkward positioning and the impact on the knees. After retirement, many goalies require knee or hip replacement surgeries. Although the butterfly style increases the potential for injury, it is still the most effective way of playing. For that reason, goalies all over the world will likely continue to use the butterfly style of goaltending.

The butterfly motion is executed repeatedly by goalies during practices and games and no further action has been taken to prevent common types of injuries or to better understand the mechanisms behind these injuries. Athletes are often forced to sacrifice their health and shorten their careers for better efficiency in games. It is believed that with a better understanding of the mechanisms of injury and new equipment technologies, potential solutions can be developed through better designed materials and equipment. The study seeks to implement a motion capture system, in conjunction with force plates, to quantify potential parameters that could increase the potential for injury, such as joint angles, joint reaction forces, and joint reaction moments.

Figure 1. Extreme valgus (knocked knee) position of the butterfly style of goaltending [1].

2.0 The Research Question

The combination of hip internal rotation, knee external rotation, and knee flexion are often identified as the main causes of common injuries among athletes. It is hypothesized that hockey goalies are likely to experience similar motions during butterfly movements. Most research done on hockey goalies has focused on the hip joint and there has been significantly less research done on the knee joint. This thesis seeks to answer the question: can we quantify the dynamics and kinematics, such as joint angles and forces, using motion capture methods to further understand the potential for injuries, such as ACL, and MCL tears?

3.0 Background Research

3.1 Introduction to the Butterfly Style of Goaltending

The butterfly style of goaltending is a technique which helps goalies cover the bottom of the net by dropping into an extreme valgus position. The butterfly style was developed in late 1960s and is by far the most efficient way of playing hockey for goalies. Most goalies learn this technique when they first start playing since it is highly effective. The butterfly motion requires goalies to move into a position that requires internal rotation of the femur, external rotation of the tibia, and flexion of the knees. It was not until recently that there have been more and more reported injuries and surgeries done on hockey goalies related to the butterfly motions. For the season of 2016 – 2017, 24% of the goalies in the National Hockey League (NHL) sustained lower body injuries.[2] Ross et al. showed that there are even goalies that have had surgery at ages as young as 14 due to hip injuries caused by these motions [3].

3.2 Introduction to Anatomical Motions Related to Butterfly Motions

The butterfly position involves internal rotation of the hip and external rotation, flexion, and abduction of the knee. Flexion is a movement in the anterior – posterior plane which decreases the angle at the joint. Extension is a movement in the anterior – posterior plane which increases the angle at the joint. Extension past the anatomical position is called hyperextension. Abduction is movement away from the longitudinal axis of the body in the frontal plane. Adduction is movement toward the longitudinal axis of the body in the frontal plane. Medial rotation, also known as internal rotation, is a movement when the anterior surface of a limb turns toward the long axis of the trunk. The opposing movement is called lateral rotation, also known as external rotation[4].

The hip joint is a synovial ball-socket joint. It is a multiaxial joint which typically allows up to 120° in flexion, 30° of extension (hyper), 45° of abduction, 30° of adduction, 45° lateral/external rotation, and 45° of medial/internal rotation. The knee joint is a synovial hinge joint. It is a uniaxial joint which typically allows 0 - 135° of flexion/extension. Any extreme form of abduction, adduction, rotation, or hyperextension could lead to injuries[5].

3.3 Dynamic Knee Valgus (DKV)

Knee Valgus, also known as knock knee, is the medial motion of the knee in the frontal plane. Dynamic knee valgus is a complex movement combination involving the hip, knee, and ankle. In the literature, DKV is defined as a combination of hip adduction, hip internal rotation, knee flexion, knee external rotation, knee abduction, and ankle inversion [6, 7]. DKV is often linked to ACL injuries and patellofemoral pain (PFP). Research has also suggested that valgus knee alignment increases the risk of lateral compartment knee osteoarthritis [8]. DKV is often a cause of injuries for athletes and the butterfly position is an extreme example of DKV. ACL, MCL, and meniscus injuries are commonly seen with athletes performing movements that result in DKV motions.

These are also the most common injuries seen among hockey goalies. Any type of injuries to the ligaments could lead to degenerative knee damage over time depending on the severity, which in the long-term could potentially lead to the need for knee replacement [9].

3.4 Femoroacetabular Impingement (FAI)

Until recently, there has not been a significant amount of research done on injuries commonly associated with hockey goalies. Most studies focus more on a specific type of hip injury called Femoroacetabular Impingement [10]. FAI (shown in Figure 1) is an uncommon injury among the general population. However, this is the most common type of hip injury for hockey goalies due to the flexion, adduction, and internal rotation of the hip. The butterfly style of goaltending requires goalies to rotate their hips internally beyond their limits causing the femur neck and the acetabulum socket of the hip bone to collide [11]. Severe cases of FAI may require surgery and sometimes even total hip replacement. Ross et al. showed that hockey goalies that use the butterfly style of goaltending have a high prevalence of cam-type FAI. Clinically, FAI for is associated with an elevated alpha angle, the angle formed between the acetabular roof and the vertical cortex of the ilium, as shown in Figure 3, and a loss of offset. The loss of offset is greater in magnitude and more lateral when compared with the angle observed for positional hockey players [3].

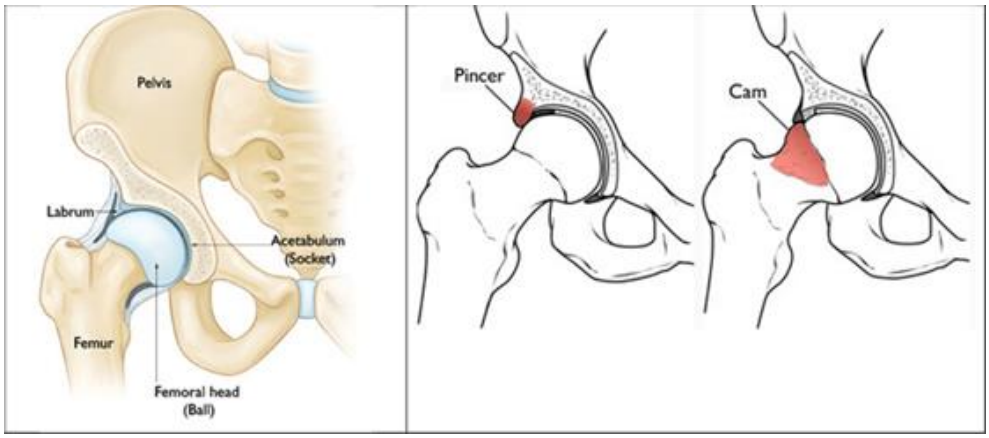

Figure 2. Impingement location of pincer type Vs. cam type Femoroacetabular Impingement [12].

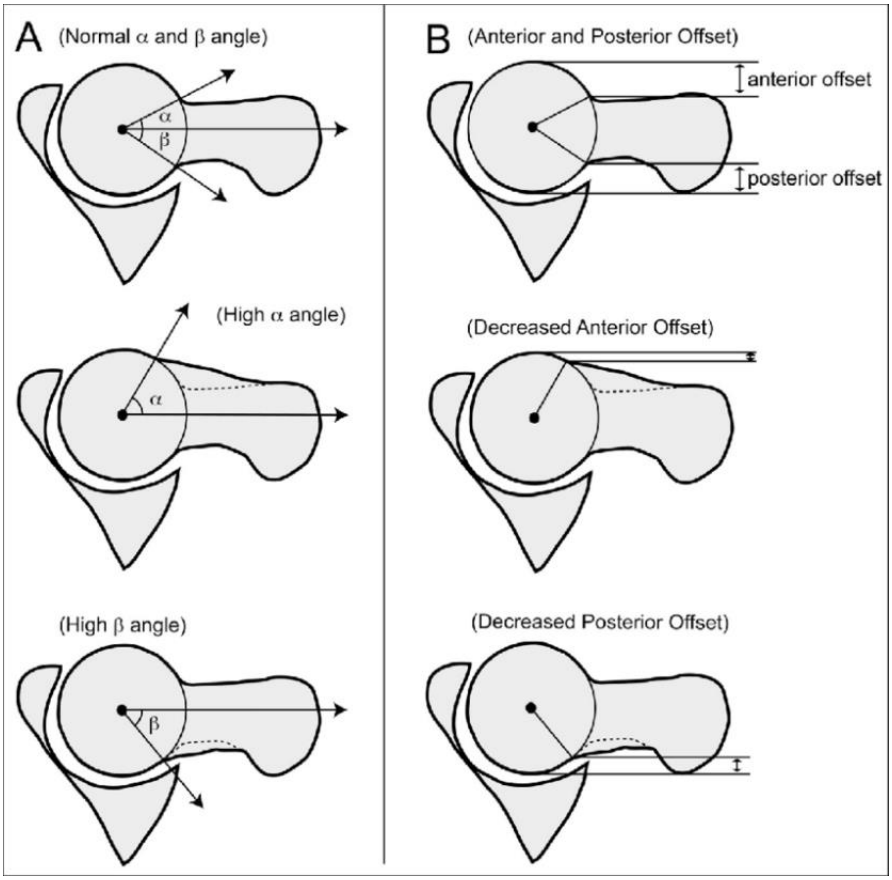

Figure 3. Normal alpha angle and beta angle and possible abnormalities [13].

3.5 Common Knee Injuries

There are four ligaments that support the knee joint. The MCL, located on the medial side of the knee, provides medial support; the LCL, located on the lateral side of the knee, provides lateral support; the ACL and PCL cross over each other and attach the intercondylar area of the tibia and the condyles of the femur. The ACL and PCL restrain the anterior and posterior movements of the tibia [4]. Ligaments and menisci tears are common sports injuries. The ACL provides anterior stability with or without loading, as shown in Figure 4 [14]. ACL injury, in particular, is one of the most common knee injuries among athletes. There are more reported cases of ACL tears in soccer players than in basketball players. Female athletes have also been reported to have a higher rate of ACL injuries, in comparison to male athletes, regardless of the sport due to the anatomical structure and influence of hormones. Out of all of the reported ACL injury cases, a greater percentage of the injuries occur in non-contact sports, which suggests that the underlying joint mechanics and dynamics likely play an important role [15]. Hewett et al. suggested a potential link between excessive dynamic valgus and the risk of ACL injuries. If an athlete is not properly aligned, he or she may be at increased risk for injury [16]. MCL injury is another common knee injury. MCL are often chosen for studies due to the high incidence of MCL injuries and the clinical importance of the MCL in restraining

valgus rotations. Su et al. showed in the results that the threshold for cyclic strain is lower than that of tensile strain, at which structural damage of the ligament would occur [17]. Repetitive movements of the joints could result in fatigue and failure of ligaments and could further cause injuries at the joint.

Studies that have looked at knee injuries specifically among hockey goalies are very limited. The knee injuries commonly seen in hockey goalies are similar to those seen in other sports and include tears of the meniscus, the ACL, or the MCL [18]. Most of these injuries occur due to DKV, as shown in Figure 5, which are associated with injuries in other sports [7]. For hockey goalies, the combined motions of the hips and knees put the ligaments under tremendous amounts of stress, causing a higher potential for injuries. The impact due to the contact of the knees and the ice is also a concern and potential cause of injuries. During butterfly motions, goalies' knees must drop to the ice in a fraction of a second, which could create large forces on the medial sides of the knees. The combination of DKV and the impact force could put goalies at a greater risk for injuries.

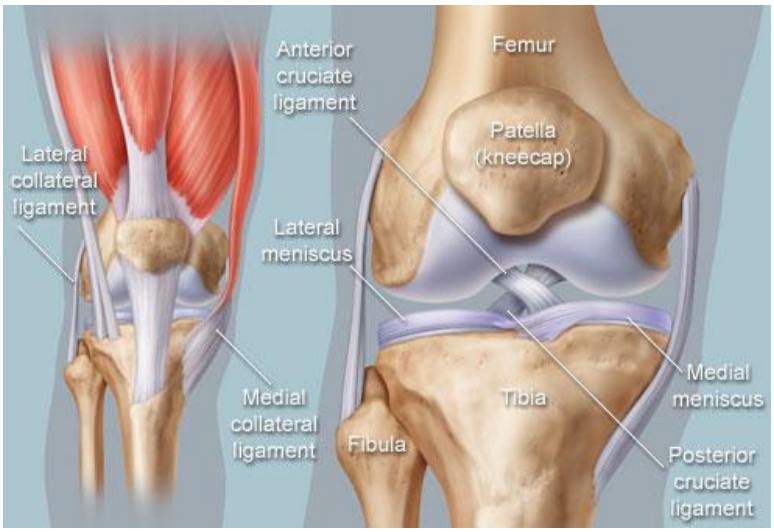

Figure 4. Breakdown of the anatomy of the knee [19].

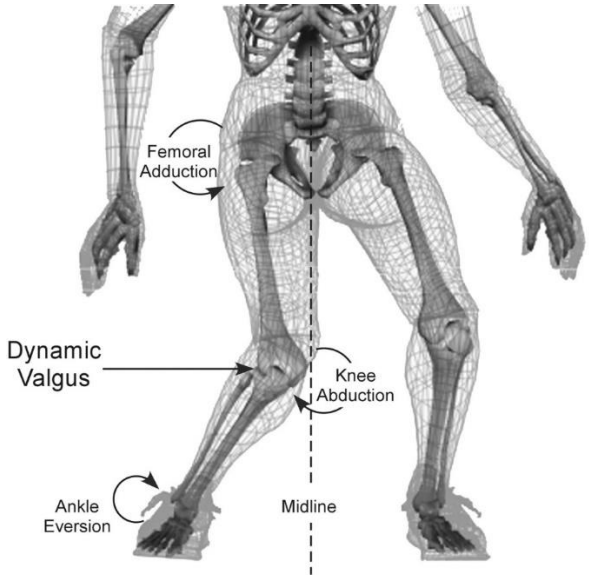

Figure 5. Motions involved in dynamic knee valgus [16].

3.6 Introduction to Motion Capture Systems

Motion capture systems are often used to obtain kinematic data. There are several different types of motion capture systems: electromagnetic, electromechanical, Inertial Measurement Unit (IMU) systems, and optical systems. The most commonly used system is an optical system. There are two primary types of optical systems, marker based and markerless. Marker based optical systems use cameras to track the movements of each of several markers, which are attached to the subject. Marker based systems have a higher level of accuracy in comparison to markerless systems. One drawback is that each marker must be seen by at least three cameras at all times. Ensuring that each marker can be seen by three cameras is nearly impossible for studies involving hockey goalies due to the size and positioning of the goalie equipment. Markerless systems use cameras to identify a subject in space then use a software program to fit a skeleton onto the subject. For hockey goalies, markerless systems can fit a skeleton onto the subject, but the systems cannot capture any movements between the subject and the equipment. Markerless systems will only capture the movements of the equipment. An Inertial Measurement Unit (IMU) is the second most commonly used motion capture system. An IMU consists of sensors with gyroscopes and accelerometers that are attached to the subject. Angular velocity and linear acceleration are captured in 6 axes and the data can be transferred wirelessly. Body position and movement (relative to a known starting position) can be determined from the kinematic data captured. Electromagnetic motion capture systems rely on the magnetic flux of three orthogonal coils on both the transmitter and each receiver. Data captured with electromagnetic systems can be very noisy because the signal can be impacted by any magnetic and electrical components in the environment. The capture volumes for electromagnetic systems are also dramatically smaller than those for optical systems.

Electromechanical systems combine potentiometers and exoskeletons to capture kinematic data, but restrict a subject's movements.

3.7 Motion Capture Used in Biomechanics Research

Motion capture is often used for biomechanics research, more specifically for studying athlete injuries. There have been numerous studies conducted with motion capture systems specifically for studying DKV in different athletes. Wolfgang et al. showed that both marker based optical systems and IMU systems can be used for identifying DKV and performed motion studies of athletes [20]. Clinically, these studies supported the notion that individuals with valgus malalignment exhibit kinematic patterns at the hip and knee that may predispose a limb to injury [21]. Wijdicks et al. studied hockey goalies using a marker based optical motion capture systems and located the markers on the back of the subject's legs and captured the images from the back. The study compared changes in the internal rotations of the hip joint and the knee impact forces when the subject was wearing pads of different widths [22]. The rotation of the joints was captured using an optical motion capture system and the forces were captured using a force plate. The results showed no significant changes in the hip kinematics when the width of the pads changed. The study did not specifically analyze correlations between the butterfly motions and the potential for hip injuries. Although the study was able to capture goalie motions using a marker-based system, the rotation of the femur and tibia could not be fully captured.

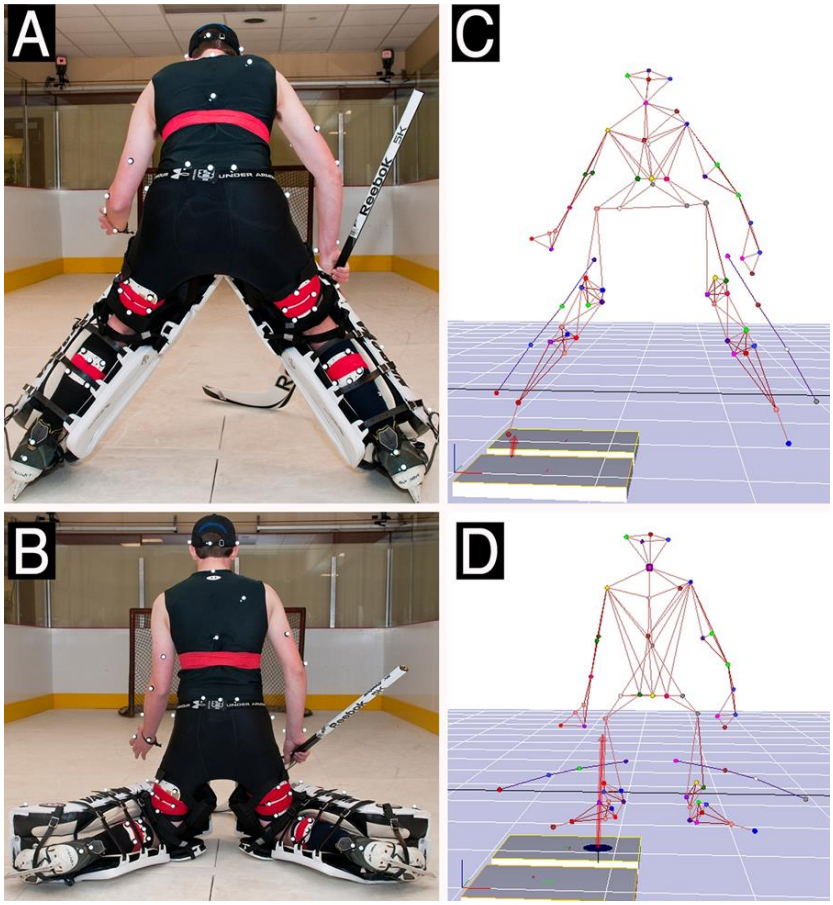

Figure 6. Image of the testing setup using an optical motion capture system from the back [22].

3.8 Comparison of Different Motion Capture Methods

Preliminary research was done to determine which types of systems would be the best for motion capture of hockey goalies. A variety of motion capture systems exist that could be used for capturing hockey goalie motions, but each have strengths and weaknesses. A preliminary comparison of the capabilities of optical and IMU systems was done. A specific comparison of two optical motion capture systems, one marker based and one markerless, is shown below in Table 1. A comparison of three of the most commonly used IMU motion capture systems is shown below in Table 2.

Type	Optical	
System	Vicon (Marker)	Kinect (Markerless)
Included	8 cameras with markers on joints	2 kinects

Pros	High frame rate	Cheap
	Wide capture space	
	Low latency	
	Can be integrated with IMU	
	Software included	
Cons	Require clear line of sight	Inaccurate
	Require power source	Low frame rate
	Expensive	Require clear line of sight
Frame Rate (HZ)	250 - 330	30
Resolution	1.3 - 2.2 MP	1 deg
Cost	$43,142.50	$200

Table 1. Comparison of optical motion capture system

Type	IMU		
System	Xsense	Synertial	MyoMotion
Included	17 inertial sensors in a suit	22 inertial sensors in a suit	7 intertial sensors
Pros	Wireless	Wireless	Wireless
	Build in battery	Build in battery	Build in battery
	High frame rate	Can increase number of sensors if needed	High frame rate
	Unrestricted of capture space	Smaller and lighter sensors	Can be integrated with Vicon
	Can be integrated with Vicon	High frame rate	
	Software included		
Cons	Higher latency	Little background information	Has a drift
	Larger and heavier sensors	Has a drift	

	Has a drift		
Frame Rate (HZ)	240	120	100 - 200
Resolution	1 deg	1 deg	1 deg
Cost	$39,000	$12,450	$20,000

Table 2. Comparison of IMU motion capture system

3.9 Optical Marker System Test

Preliminary tests, shown in Figure 4, were done with a regular camera and tape on the subject to simulate a marker based optical motion capture system, such as the Vicon system presented in Table 1. The goal was to determine if the markers remained visible during a butterfly motion since, in full optical systems, one marker must be seen by at least three cameras at once. A piece of blue tape was put onto the lateral tibial condyle of the subject as if it were a marker for the motion capture system. From the preliminary test, the only location in which the camera could capture the position of the tape when the subject was performing butterfly motions was directly from the top due to the rotation of tibia. Using an inertial motion capture system or a markerless optical system instead of a marker-based system was determined to be preferable since these systems could bypass the limitation in which the equipment obscured the views of the joints.

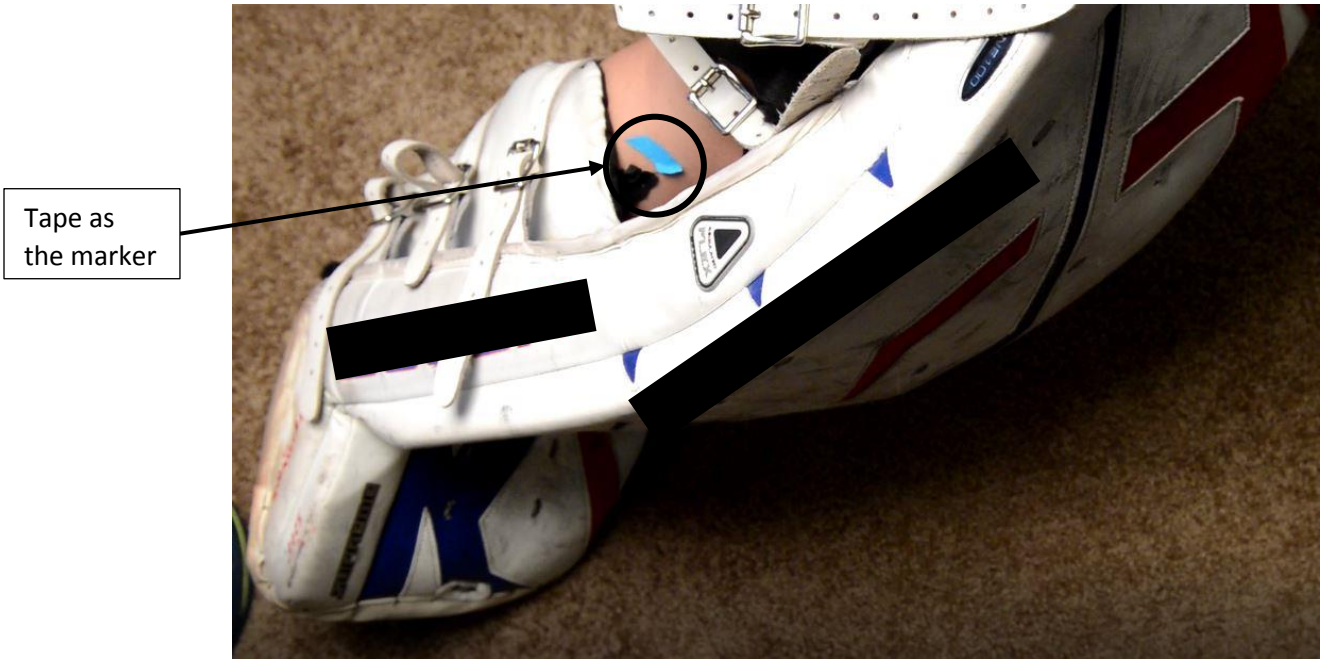

Figure 7. Preliminary test for line of sight when the subject is in a standing position. The blue tape represents one of the required locations for the reflective markers for an optical system.

Figure 8. Preliminary test for line of sight when the subject is down in a butterfly position. The blue tape represents one of the required locations for the reflective markers for an optical system.

3.10 Microsoft Kinect Test

The Microsoft Kinect (Microsoft, Ramond, WA) is a camera-based motion sensing device with a depth sensor that allows the system to sense motion in 3D. Microsoft Kinects were used in a preliminary test to assess the feasibility of using a markerless system. Two Kinects were used for the test. One was placed at the front of the subject and the other at the rear of the subject. The subject performed several butterfly motions. The motion was captured using two different camera configurations. One configuration positioned the main Kinect in the front and the other configuration positioned the main Kinect in the back. Data captured using the Kinects shows the general butterfly motion, but could not capture rotational motions. In Figures 8 and 9, the two images should show the same motions. However, the Kinect image showed little resemblance to a butterfly position. The Kinect also required some time to adjust the position of the subject after the movement was already performed. In addition, the frame rate of the Kinect was not enough to capture the complexity of the motions and the system software had difficulty interpreting the complex movements associated with the butterfly position since they were not expected anatomical positions.

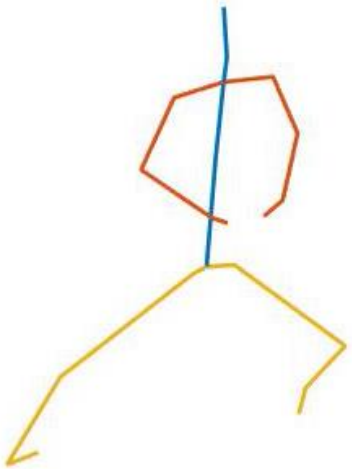

Figure 9. Capture positions results from the Kinect test generated by MATLAB.

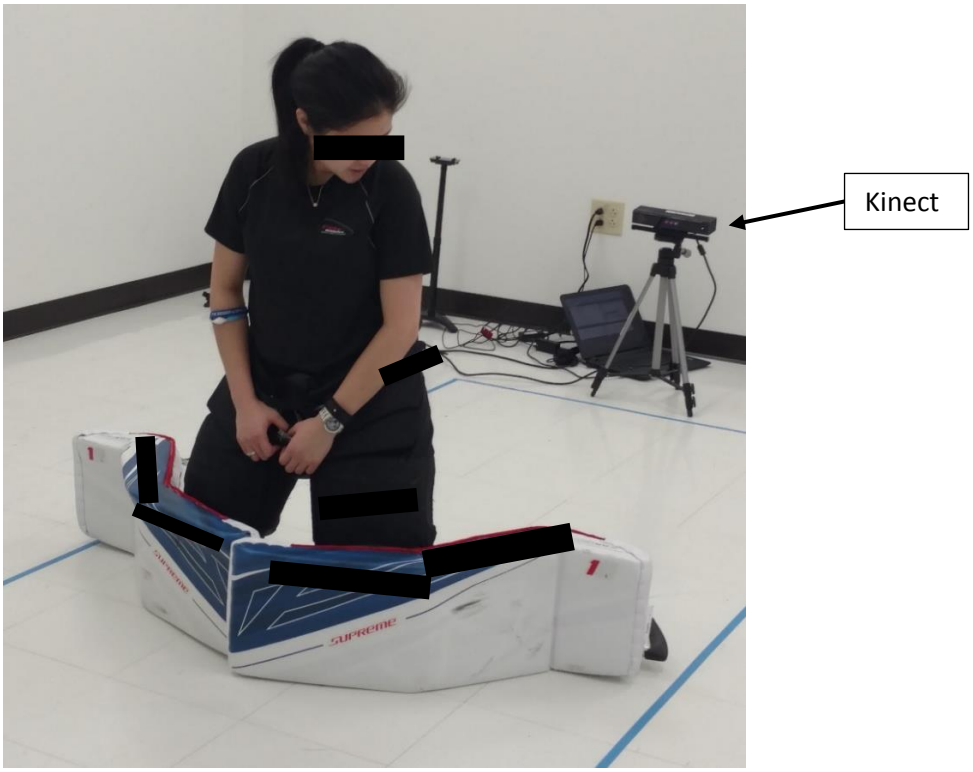

Figure 10. Lab setup for the preliminary test using the Kinect system.

3.11 Feasibility of Optical Systems

Based on the results from the preliminary tests using both a marker based and a markerless optical system, it was concluded that, for the purposes of this thesis, optical systems were not suitable for capturing the complexity of butterfly movements in goalies wearing full equipment due to the requirement for line of sight. However, an optical system could be used for supplemental confirmation of the validity of data obtained from an IMU system or other motion capture methods.

3.12 The Xsens Inertial Motion Capture System

Optical motion capture systems were eliminated based on the preliminary results from the line of sight test. Without a line of sight, the cameras for an optical motion capture system would not be able to track the markers and could result in large errors or missing data. The advantages of various IMU systems are shown in Table 2. The Xsens MVN Awinda inertial motion capture system (Xsens Technology, Enschede, Netherlands) was chosen for this study because of its portability, setup procedure and time, and prior validated use in other biomechanical research studies.

The Xsens MVN Awinda is an IMU motion capture system. The system includes 17 wireless IMU sensors, which consists of a gyroscope, accelerometer, and magnetometer, an Access Point (AP), Velcro strips, a software dongle license, chargers, connection wires, and a backpack for holding components. The software used for Xsens data capturing is Xsens Analyze. The software can be downloaded from the Xsens website and the dongle license must remain inthe Xsens backpack along with the AP, which handles data between the sensors and computer, and the IMU sensors. After starting the software, anthropometric measurements need to be input before starting a new capture. While the software is being prepared for capture, sensors must be strapped onto the subject at the locations suggested by the manufacturer. After all sensors are on the subject, a calibration needs to be done. The calibration requires the participant to stand in the N-pose, in which a subject stands straight up with their arms on the lateral sides of the thighs. The subject must remain in the pose for a few seconds then walk forward in a straight line for a few steps before turning around and walking back to the initial location. After the calibration, the subject needs to stand still for approximately 30 seconds to warm up the filters. If required, the subject can face the desired global x-axis direction before clicking the “Apply calibration” button.

After a calibration is applied, capture can begin. The Xsens Analyze software saves the capture files as .mvn files that can only be opened in the Xsens software. To further process the data, Xsens provides options to export the data files as .mvnx, .c3d, .fbx, or .bvh files.

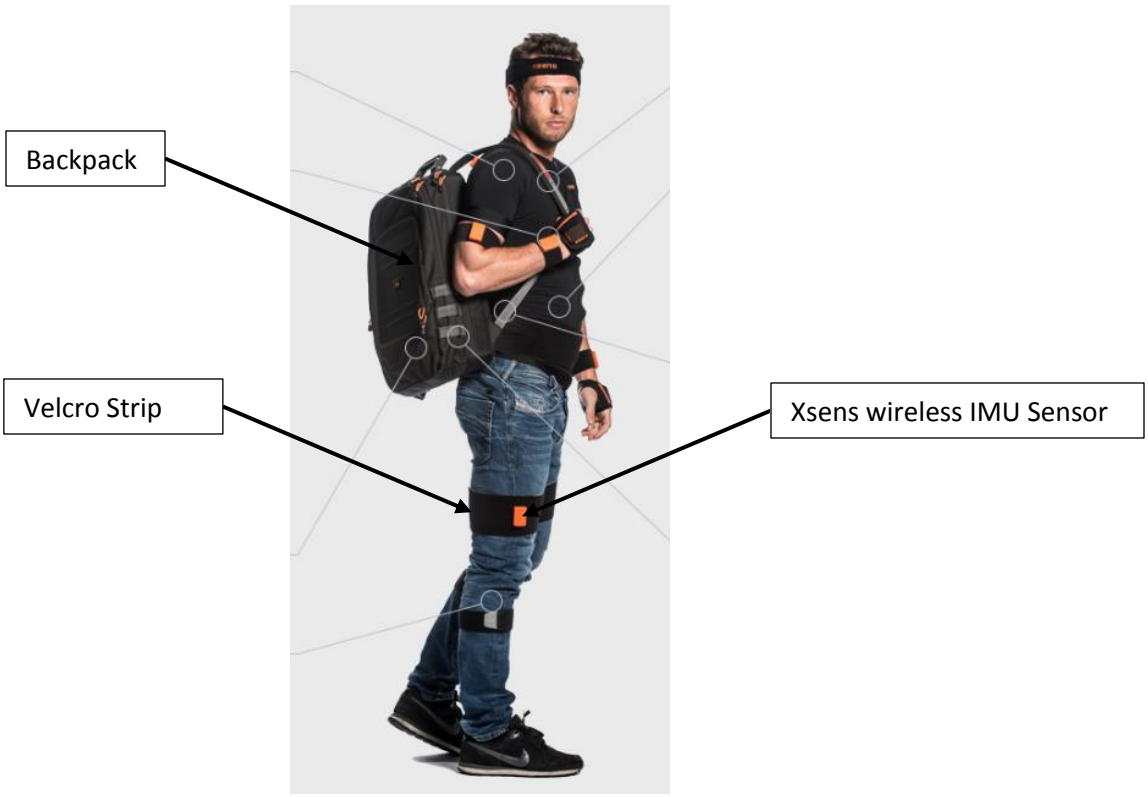

Figure 11. The Xsens MVN Awinda IMU system. The system consists of 17 wireless IMU sensors, Velcro strips, and a backpack.

3.13 Importance of the Thesis Study

Multiple studies suggest that there is a strong relationship between DKV and various hip and knee injuries. However, no comprehensive studies have been done to look at DKV and knee injuries in hockey goalies. The potential for injuries in hockey goalies is likely higher than for other athletes due to the extreme DKV movements associated with the butterfly motions. However, no complete studies have been done on the topic due to limitations in motion capture as a consequence of the needed, bulky goalie equipment and the complex movements associated with the butterfly position. It is believed that such a study could be beneficial for understanding the potential for injury in hockey goalies as a consequence of DKV. The study could also benefit future studies for other sports with similar equipment and movement complexities.

4.0 Methods

The Xsens MVN Awinda was the motion capture system used in this study. The testing procedures were separated into two parts, kinematics and kinetics. The kinematic part was done on the ice with full equipment using just the Xsens MVN Awinda. The kinetic part was done in the lab with full equipment, except for the skates, using the Xsens MVN Awinda as the motion capture system and AMTI force plates along with a Vicon Nexus Lock+, a device that synchronize all different data collection instruments, for data incorporation.

4.1 Subject

All tests for this study were done by one subject. Human subject IRB approval was obtained and is included in Appendix K. The subject for the study was a 23-year-old female hockey goalie that plays hockey at a competitive level internationally. The subject is 166 cm in height and weighs 53 kg with no prior surgeries or injuries on the hip, knee, or ankle joints.

4.2 Placement test to Assess Placement of the Xsens Lower Leg Sensors

For IMU systems, drift is often a large source of error. For this particular study, it was expected the impact time and the time of the motions would be so short that any drift effects would be limited. However, a series of data captures and analyses were performed to verify the repeatability of the system for capturing hockey goalie motions.

The IMU sensors were placed on the subject according the Xsens instructions except for the lower leg sensors (See Table 3 for Xsens recommended sensor locations). The Xsens recommendation is that the lower leg sensors should be placed on the medial side of the leg. However, due to the motion that is being investigated, there was a potential for damaging the sensors and injuring the participant during impact events. The decision was made to place the lower leg sensors on the lateral side of the leg to minimize the possibility of damage or injury. Further testing was done to justify this decision by doing two different captures. One capture placed the sensors on the medial side of the lower leg and the other placed the sensors on the lateral side of the lower leg. Calibrations were done between each capture to limit other factors which could affect the results, such as changes in the lower leg sensor locations. The subject performed 3 sets of butterfly motions without impacting the floor at high velocities or forces. The results from the test, shown in Section 5.1, showed no significant differences between the joint angles obtained for the lower body.

Location	Optimal Position
Foot	Middle of bridge of foot
Lower Leg	Flat on the shin bone (medial surface of the tibia)
Upper Leg	Lateral side above knee

Pelvis	Flat on sacrum
Sternum	Flat, in the middle of the chest
Shoulder	Scapula (should blades)
Upper Arm	Lateral side above elbow
Fore Arm	Lateral and flat side of the wrist
Hand	Backside of hand
Head	Any comfortable position

Table 3. Xsens recommended sensor locations.

4.3 Xsens Repeatability and Data Analysis Method Test

A trial was defined as one butterfly movement and a capture was defined as the data collection period from the start of the motion capture to the stop of that same capture period. A capture could include one or multiple trials. Two captures were done for one subject to assess the repeatability of the system. The subject performed 3 butterfly movements during each capture using full body Xsens sensors. The joint angles for the two trials from each capture were plotted against the percent completion of the butterfly movement versus time. On this scale, 0% was defined as the initiation of the butterfly motion and 100% was defined as when the participant was standing on both legs after recovery. The start and end points for the drop and recovery of the motion were identified by looking at the motion and the changes in joint angles in Xsens Analyze. T – tests were performed for the maximum joint angles from the different trials and the two captures. The results from the T-tests are described in Section 5.2

4.4 Range of Motion Tests

Passive and active ranges of motion for the hip, knee, and ankle joints were measured by a professional physical therapist following the standard protocols for range of motion tests. The tests performed included:

Hip	Flexion	Extension
	Abduction	Adduction
	Internal Rotation	External Rotation
Knee	Flexion	Extension
	Varus Test at 0 deg flexion	Valgus Test at 0 deg flexion
	Varus Test at 30 deg flexion	Valgus Test at 30 deg flexion
Ankle	Dorsiflexion	Plantarflexion
	Inversion	Eversion
	Subtalus Inversion	Subtalus Eversion
Any difference from the anatomical 0 at rest for all three joints		

Table 4. Ranges of motion tested.

The knee varus and valgus stress tests were positive and negative tests with negative meaning the individual's knee ligaments are fully intact with no apparent

injuries. All other ROM tests were measured in degrees. The results from the test are described in Section 5.3.

4.5 On-Ice Data Collection Tests to Obtain Joint Angles

The data captured for the study was obtained in two parts, kinematic (on-ice) and kinetic (in lab) using force plates. The kinematic part was used for obtaining joint angles and other kinematic data. To limit any outside factors that could potentially change the motion of the subject, the data collection was done on the ice with full equipment. Anthropometric measurements, required as inputs to the Xsens, were taken prior to data collection. The measurements required are shown in Table 5.

Measurement	Definition
Body Height	Floor to the top of the head
Foot Length	Back for the heel to the front of the toe (with shoes)
Arm Span	Fingertip to fingertip (T-pose)
Ankle Height	Floor to the center of the ankle
Hip Height	Floor to greater trochanter
Hip Width	ASI to ASI
Knee Height	Floor to lateral epicondyle
Shoulder Width	Distance between left and right acromion
Sole Height	Floor to the sole of the foot

Table 5. Anthropometric measurements required by the Xsens software.

After the anthropometric measurements were done and recorded in the Xsens Analyze software, an N-pose with a walking calibration was performed. To obtain a better fit of the skeletal model for the calibration, no equipment was worn by the subject except for the skates. The foot sensors were also taped to the feet to limit any movement. After calibration, the subject performed 10 butterflies per capture for 3 captures on the ice with no stopping between each butterfly. The collected data were loaded into MATLAB for further processing. A MATLAB script, included in Appendix A, was developed from the MATLAB tool kit obtained from Xsens website to extract the maximum joint angles for the hip and knee joints for each butterfly movement from the .mvnx files saved from the Xsens Analyze software. The maximum joint angles for each butterfly were separated into a dropping portion, which described the initiation of the butterfly to when the goalie was in a full butterfly position on the ice, and a recovery portion, which spanned from the initiation of recovery to when the subject was fully standing. The initiation of dropping and recovery were identified by finding the peaks in the right hip flexion and abduction angles, respectively, as illustrated below in Figures 12 and 13.

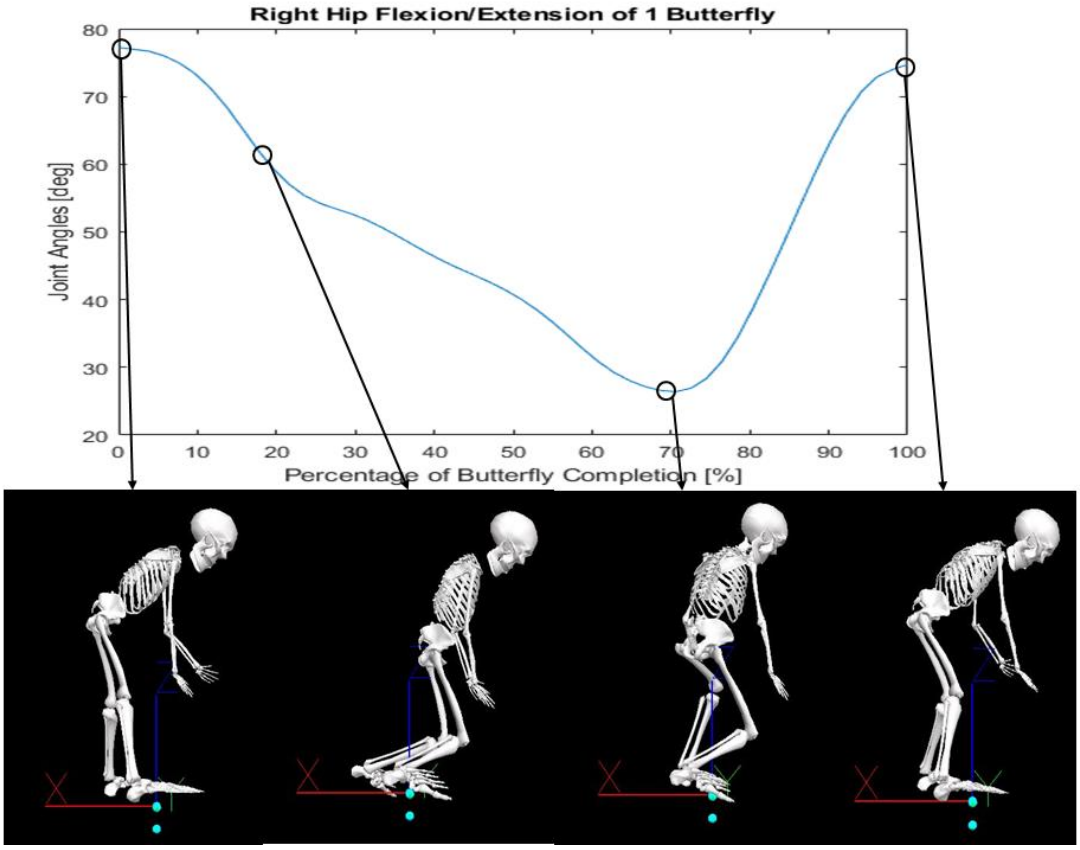

Figure 12. Hip flexion and extension angles of the right hip for one butterfly movement.

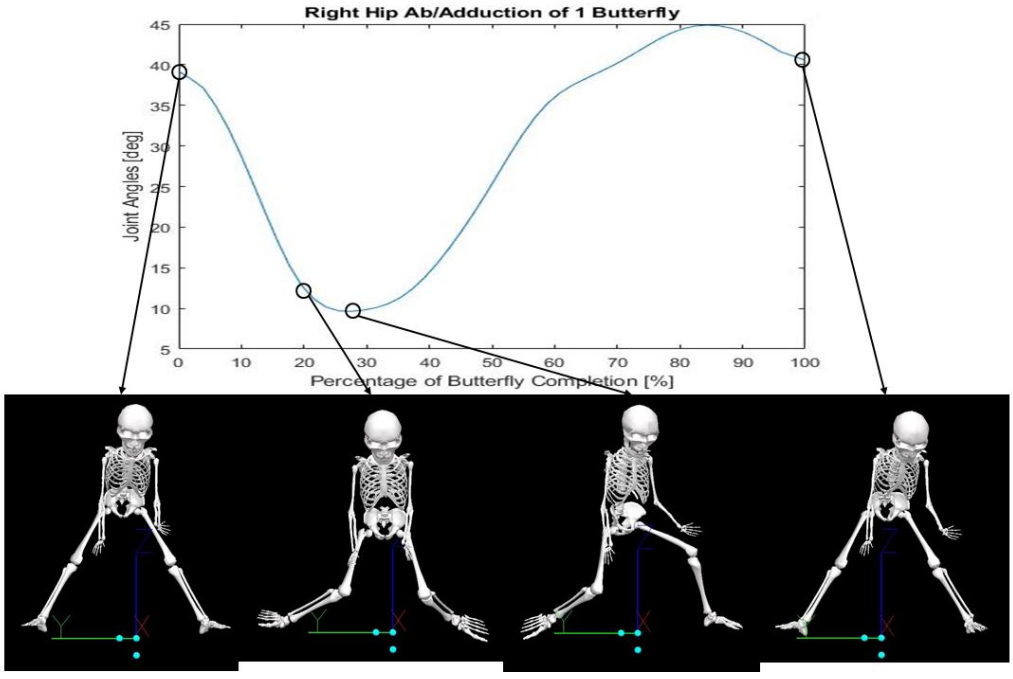

Figure 13. Hip abduction and adduction angles for one butterfly movement.

All joint angles were output based on the local coordinate system with positive X going forward, Y going up (from joint to joint), and Z going to the right. The positive and negative directions on each axis represent different joint motions. For example, positive values along the Y axis would represent internal rotation while negative values along the Y axis represent external rotation. Another MATLAB script, provided in Appendix B, was written to perform further statistical analysis on the maximum joint angles (both maximum and minimum from the same axis) and the individual's range of motion. The outliers for the maximum joint angles were identified by setting the upper and lower limits of the acceptable data to be the average ± 2*standard deviations. All of the data that were within this range were then averaged and the standard deviations were calculated. The maximum average joint angles for each motion were compared to the passive and active ranges of motion and are shown in Section 5.4.

4.6 In Lab Data Collection for Inverse Dynamics Calculations

To obtain the joint reaction forces and moments, an inverse dynamics analysis was performed. Force plates were used to obtain the load inputs required for inverse dynamics. Since the force plates are not mobile, the force testing was done off-ice. Three force plates, two AMTI OR6-6-OP-1000 and one AMTI BP600900-1000 (Advanced Mechanical Technology Inc., Watertown, MA), were used. The force plates were connected to a Vicon Nexus Lock+ box for combined data capturing. The Xsens data cannot be captured with the Vicon Nexus, so the Xsens Analyze software was still used to capture the Xsens data. A duration signal was sent from the Vicon Nexus Lock+ to the Xsens signal receiver to sync both systems together. The setup of the force plates, Vicon Nexus Lock+ and Xsens signal receiver are shown below in Figures 14 and 15.

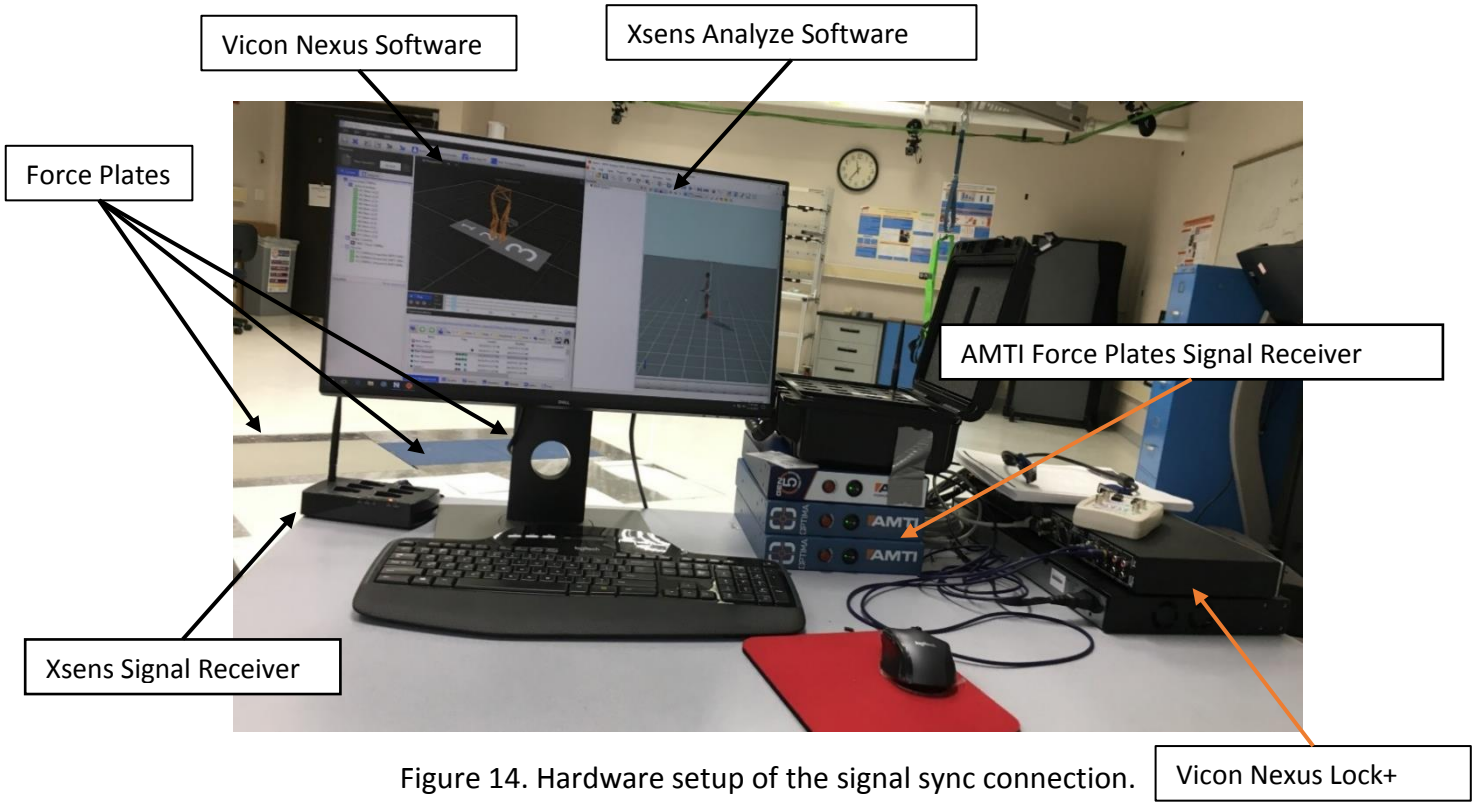

Figure 14. Hardware setup of the signal sync connection.

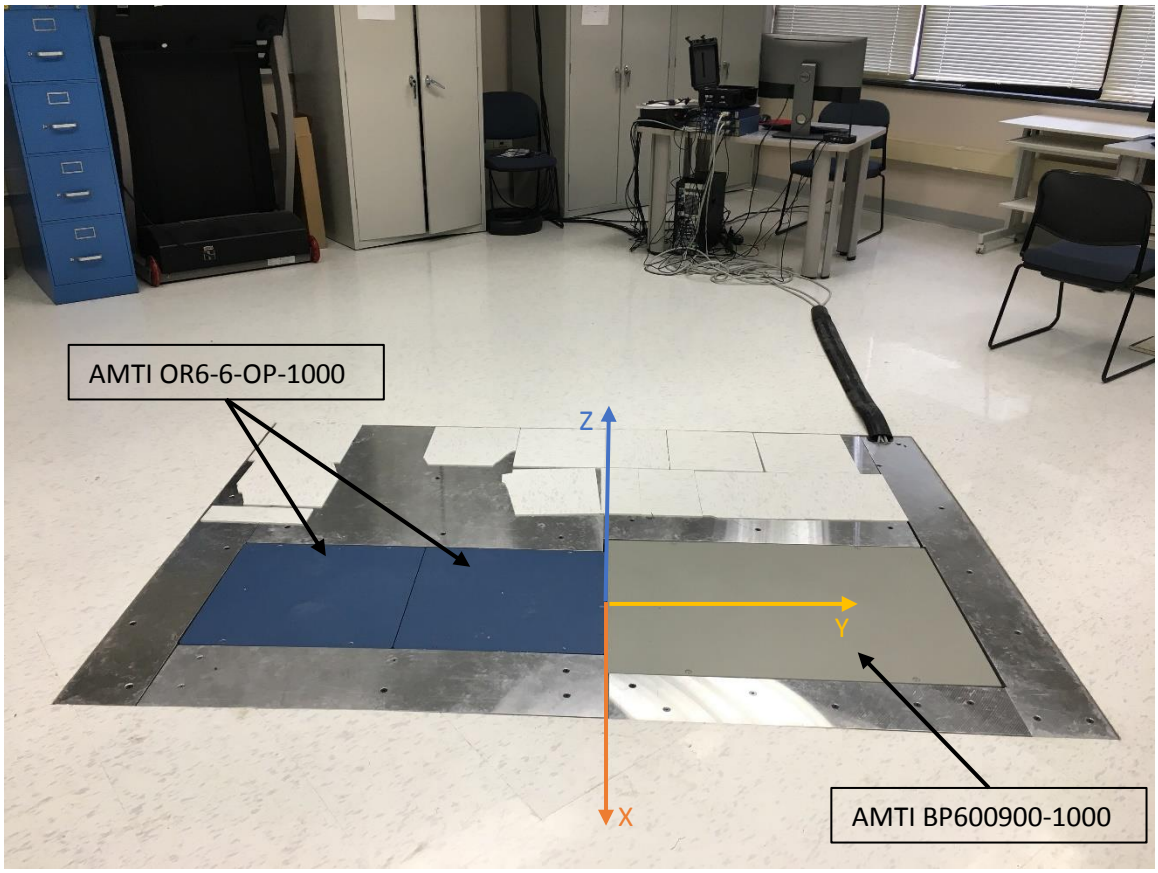

Figure 15. Setup of the force plates and the global coordinate system. The X-axis is indicated using orange, the Y-axis is indicated using yellow, and the Z-axis is indicated using blue and projects vertically upwards.

The Xsens sensor positions on the subject for this portion of the testing were the same as the locations used for the on-ice captures. The subject was not wearing skates for this portion of the testing. Based on the sensitivity of the kinematic model, it is suspected that having the skates on could introduce a large error due to the variation between the location where the force is applied and the center of pressure, COP, position output from the force plates. The subject was also having trouble maintaining balance to complete the task due to a lack of friction between the skate guards and the force plates. Although not having the subject wear skates might slightly alter the butterfly motion, this was assumed to introduce less error into the system because inverse dynamic models are highly sensitive to the location of the force being applied at the most distal segments. The anthropometric measurements were changed to account for the different sole height. Since the force plates and Xsens were running on different systems and different software, it was important to have the two coordinate systems match for the inverse dynamic calculations. It was noticed that the Xsens coordinate system would rotate even if the position of a single sensor was slightly altered. Therefore, the calibration for this test was done after all the equipment was put on to

limit any possible movement of the sensors when the subject was putting on the equipment.

The Xsens system defines the origin of the system at the back of the right heel. After the calibration process, the participant was asked to face the X-axis and locate the right heel at the origin of the lab global coordinate system, as shown in Figure 15, to synchronize the two coordinate systems. The participant was then asked to perform butterfly movements on the force plates with one leg on the AMTI BP600900-1000 and the other one on the two AMTI OR6-6-OP-1000 force plates. During the first few captures of the test, a significant change in the position of the subject in the global in the software and the capture data was noticed. By the end of the fifth butterfly performed, the subject's location in the software was no longer on the force place even though the movement was done at the same location in the lab space. It is suspected that drift was the cause of the problem. To overcome this limitation, only one butterfly was performed per capture. Five different trials were done along with one trial of normal walking and five trials of single leg squats with the same sensor locations and calibrations redone between movements.

Figure 16. Front and side view of the test markers for single leg squat movement captures.

Figure 17. Subject performing a single leg squat test using the Xsens and Vicon systems.

The .mvnx files saved from the Xsens Analyze software were directly loaded into Visual3D (C-Motion Research Biomechanics, Germantown, MD), an inverse dynamics software. Although .c3d files are generally the file format used for inverse dynamics software, .mvnx files were used in this case because the .mvnx files contained segment information. By loading .mvnx files in Visual3D, segments arepredefined, which could further increase the accuracy of the results. The force plate data was output from the Vicon Nexus as .ascii files and loaded into MATLAB for further processing. A MATLAB script, included in Appendix C, was written to load the .ascii files and separate the data from the 3 force plates into 3 different matrices. Each of the matrices had 6 force channels (F_x, F_y, F_z, M_x, M_y, M_z). The data was further resampled since the force plates were capturing at 1000 Hz and the Xsens system was capturing at 60 Hz. Visual3D can only down-sample signals if the analog frequency is an integer multiple of the motion capture sampling rate. After the resampling, the MATLAB script saved the force plate data from the AMTI BF600900-1000 into a different .ascii file. The .ascii file was imported into Visual3D with the corresponding .mvnx file using the “Import Analog Signals From AMTI Ascii File” command. After the analog data was imported, the force plate parameters needed to be input and the 6 loads from the analog signals were

assigned to the proper channels. The parameters required for the force plate are shown in Figure 18. After the parameters and signals were properly assigned, the force plate was auto-generated in the .c3d format in Visual3D, V3D. Forces were then assigned onto the proper segments for inverse dynamics.

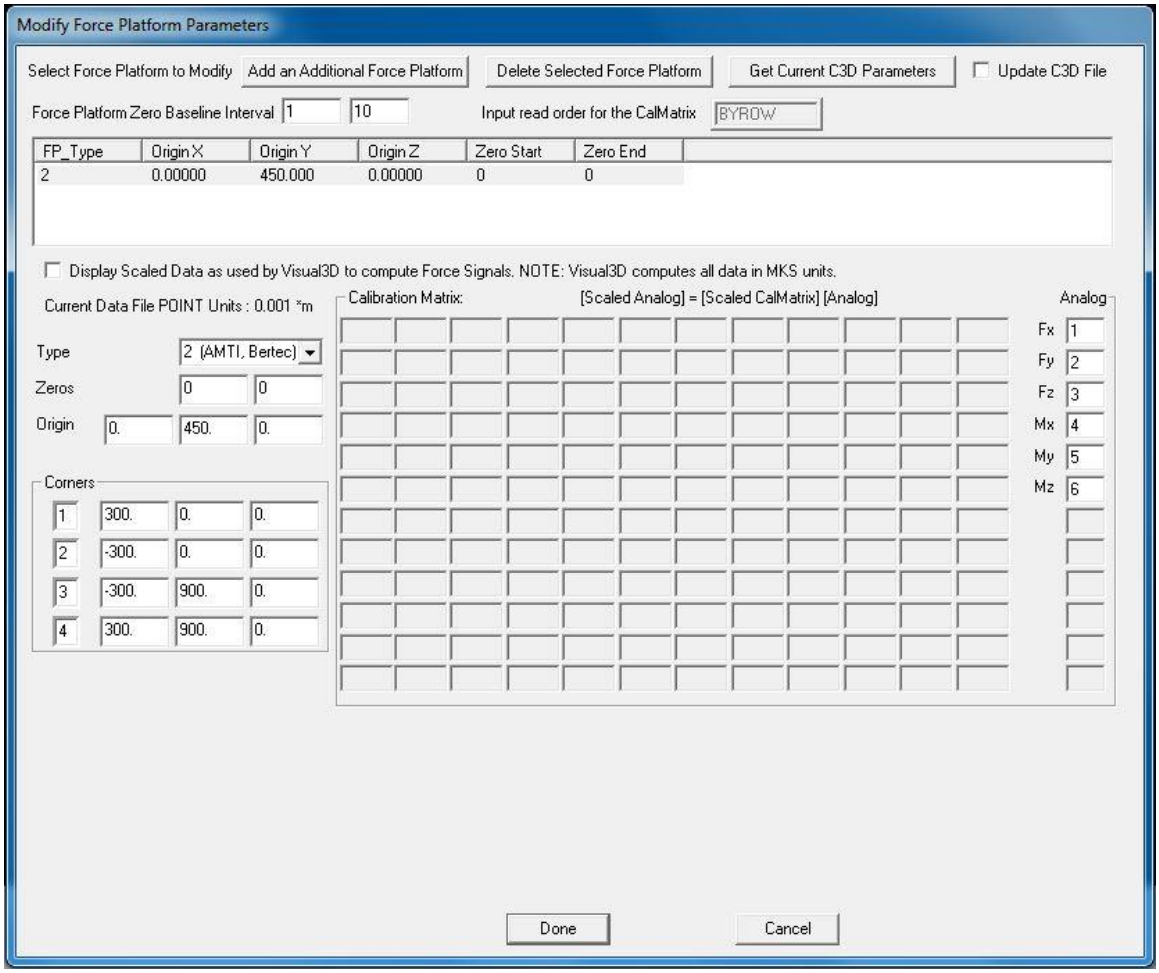

Figure 18. Force plate parameter modification window.

Visual3D can easily calculate the joint reaction forces and moments once the forces are properly defined and assigned to the segments using the “Compute Model Based Data” command pipeline. The joint reaction forces and moments of the right hip and knee were calculated for butterfly, normal walking, and single leg squat motions. The single leg squat and walking data used were from the Vicon .c3d file instead of the Xsens .mvnx file to limit any error introduced during the post processing of the force plate data since all of the force plate information already existed in the Vicon .c3d file. The computed data were then exported into .ascii files and imported into MATLAB for further processing. The MATLAB script, shown in Appendix D, was developed to find the maximum loads on the hip and knee joints during all three motions. The maximum joint reaction forces and moments for the butterfly motion were found during the dropping

process, prior to the impact and contact with the floor, since the impact would complicate the kinematic system and the actual joint loads cannot be predicted through inverse dynamics. The impact point was identified by finding the absolute maximum of the vertical force, F_z, from the force plate. The maximum loads found for all five trials of the butterfly and single leg squats were averaged, and the standard deviations were found. The maximum loads from all three motions were then compared and the results are shown in Section 5.5.

5.0 Results

This section includes results from the preliminary validation of the system and the results for the ROM, kinematic, and kinetic tests. The final results are presented in Sections 5.4 and 5.5.

5.1 Results from test to Verify Placement of the Xsens Lower Leg Sensors

Figures 19 and 20 show the joint angle results obtained from the butterfly motions with different lower leg sensor placements (medial vs. lateral). In Figures 19 and 20, the joint angles seem to be 5-10 degrees higher for knee abduction, but 5-10 degrees lower for external knee rotation when the sensors are placed on the lateral side of the leg. Based on the results from this test, some error was introduced into the results, however, to protect the sensors from impact and the wearer from injury, the sensors must be placed on the lateral side of the leg. The results from this test, showing the motions of the other joints, are shown below in Appendix E.

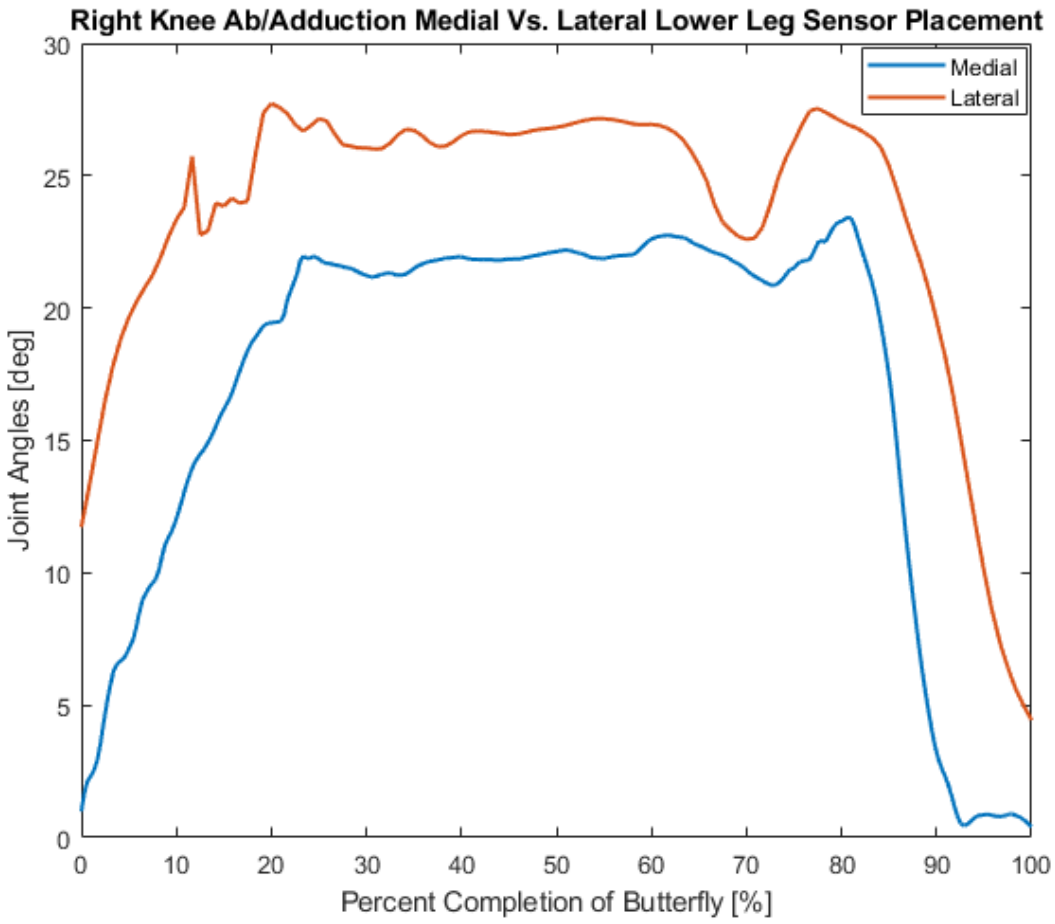

Figure 19. Right knee abduction/adduction joint angle of a single butterfly with the lower leg sensors placed on the medial side (Blue) and the lateral side (Red) of the leg. The positive direction shows abduction and the negative direction shows adduction.

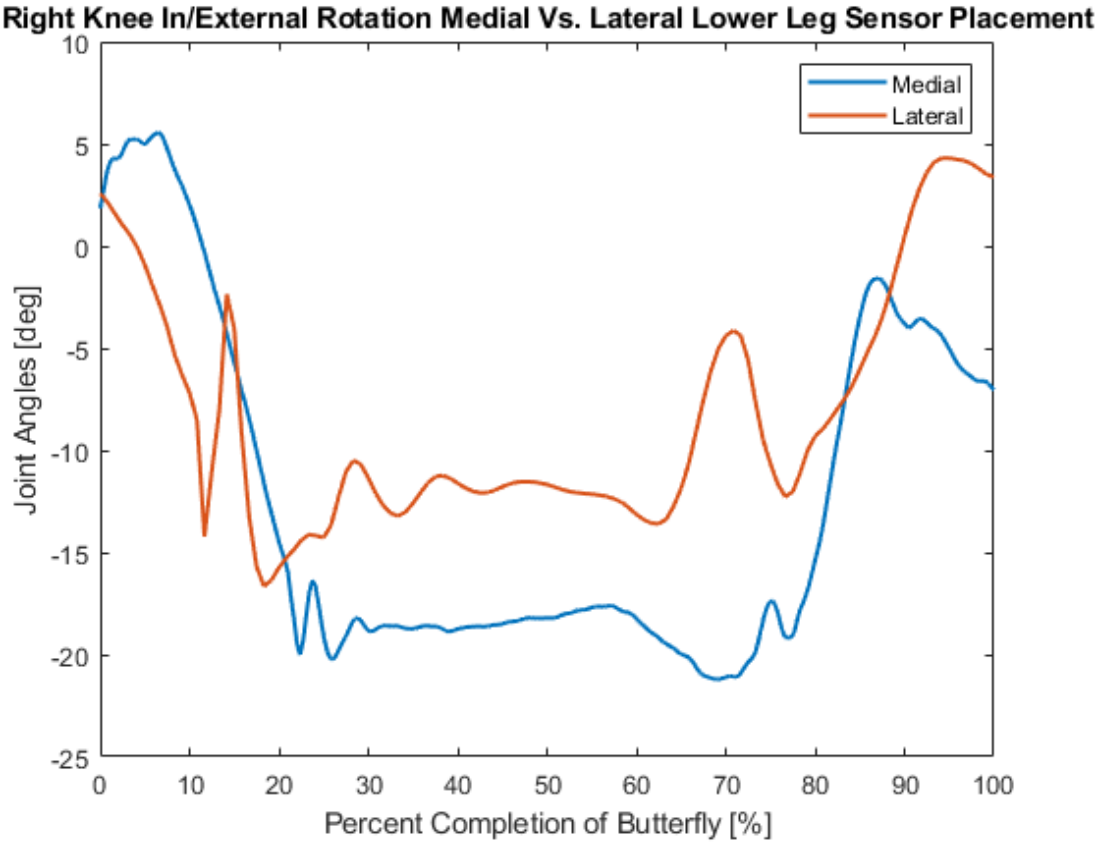

Figure 20. Internal/external rotation of the right knee during a single butterfly with the lower leg sensors placed on the medial side (Blue) and the lateral side (Red) of the leg. The positive direction shows internal rotation and the negative direction shows external rotation.

5.2 Results from the test to Determine Repeatability and Optimal Data Analysis Methods

The results from the repeatability test, shown in Figure 21, suggest that the measurements of rotation joint angles are repeatable and within 5 degrees of difference between trials. However, in looking at Figure 22, the results from trial 4 are not consistent with the other trials. In Figures 21, 22 and Appendix F, trials 1 and 2 are from the first capture after calibration and trials 3 and 4 are from the second capture. From Figures 21 and 22 and Table 6, it can be seen that the results are more consistent if they are captured in the same capture and that long capture processes without recalibration can lead to inconsistent data. The results for the other joint motions are shown in Appendix F.

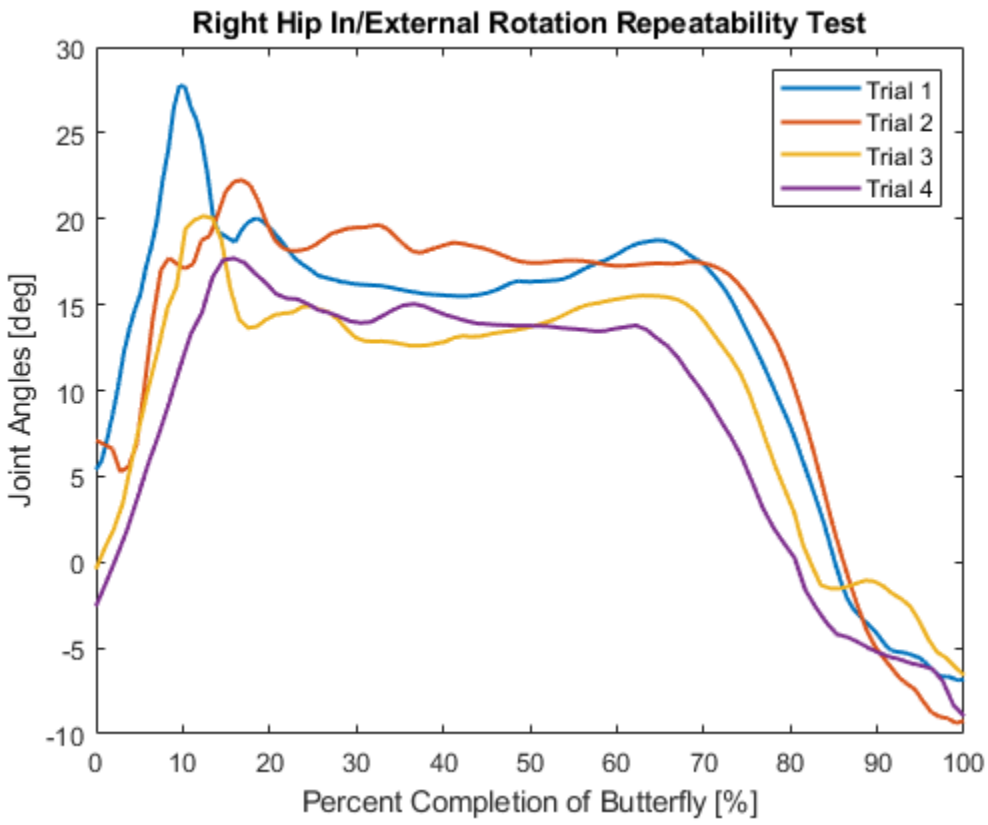

Figure 21. Internal and external rotation of the right hip for one butterfly with four different trials. Trials 1 and 2 are from the same capture and 3 and 4 are from the same capture. Positive values describe internal rotation and negative values describe external rotation.

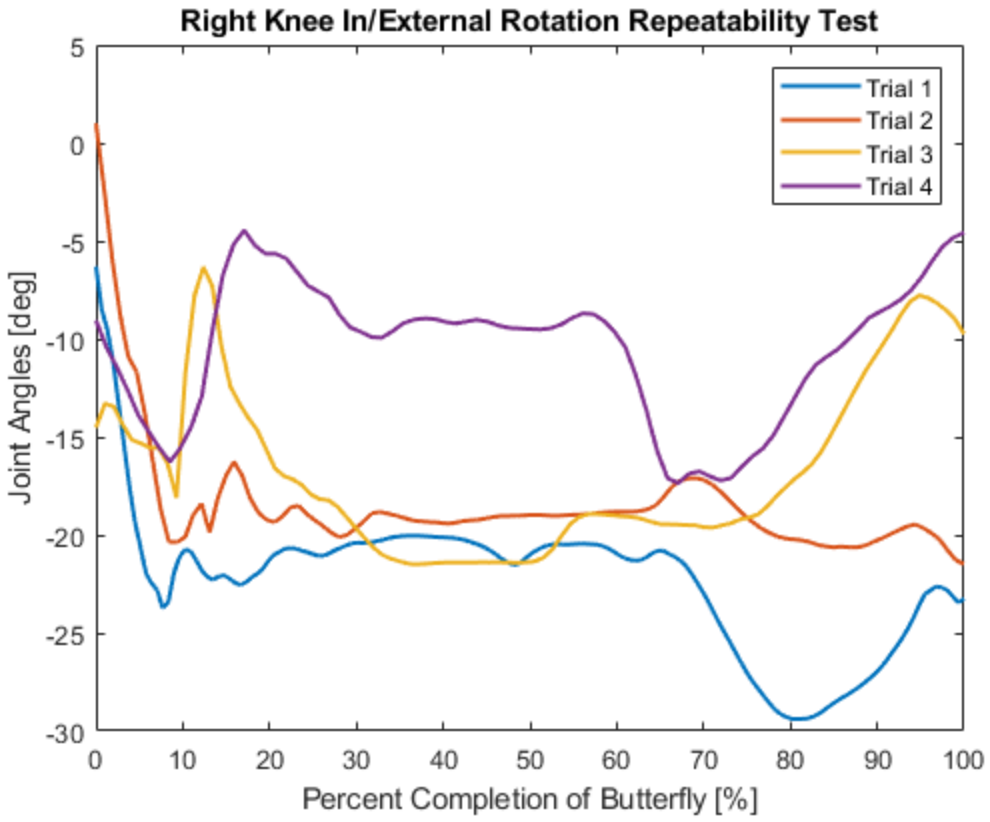

Figure 22. Internal and external rotation of the right knee for one butterfly with four different trials. Trials 1 and 2 are from the same capture and 3 and 4 are from the same capture. Positive values describe internal rotation and negative values describe external rotation.

Joint Motion	p-value between trials	p-value between captures
Right Hip Abduction/Adduction	0.0675	0.3129
	0.0011	
Right Hip Internal/External Rotation	0.001	0.0469
	0.0017	
Right Hip Flexion/Extension	0.0684	0.3321
	0.0163	
Right Knee Abduction/Adduction	0.0087	0.8579
	0.0012	
Right Knee Internal/External Rotation	0.5792	0.2388
	0.0052	
Right Knee Flexion/Extension	0.0006	0.0459
	0.0016	
Left Hip Abduction/Adduction	0.0929	0.1601
	0.0014	

Left Hip Internal/External Rotation	0.0258	0.21
	0.0018	
Left Hip Flexion/Extension	0.0831	0.033
	0.0025	
Left Knee Abduciton/Adduction	0.0015	0.0483
	0.0047	
Left Knee Internal/External Rotation	0.0027	0.0494
	0.3491	
Left Knee Flexion/Extension	0.0008	0.1499
	0.0044	

Table 6. P-values for the maximum joint angles of 1 butterfly between each trials of butterfly movements in the same capture and two trials of butterfly movements from the two different captures

5.3 Range of Motion Test Results

The ranges of motion tested were separated into an active ROM and a passive ROM. Active ROM is the ROM that can be performed by an individual without any help or restrictions from outside factors. Passive ROM is the ROM performed by a therapist without any effort from a participant. The passive ROM is limited by an individual's bone structure. The results from the range of motion test are shown in Table 7. The valgus and varus stress test results for the knees are all negative for both 0 degrees and 30 degrees of knee flexion, meaning there is no apparent knee ligament injury observed. The stress test is done to test for damage to the ligaments, more specifically the MCL and LCL. Negative values indicate that both ligaments are intact with no apparent damage. The subject also has 11 and 9 degrees of inversion at the right and left ankle and 6 and 4 degrees of genu valgum at the right and left knee, respectively, at rest.

		Active ROM		Passive ROM	
		Right	Left	Right	Left
Hip	Flexion [deg]	125	122	136	142
	Extension [deg]	9	11	9	13
	Abduction [deg]	30	18	35	31
	Adduction [deg]	11	18	25	16
	Internal Rotation [deg]	50	40	40	40
	External Rotation [deg]	30	32	56	42
Knee	Flexion [deg]	138	144	144	148
	Extension [deg]	6	5	9	8
Ankle	Dorsiflexion [deg]	10	10	11	12
	Plantarflexion [deg]	60	55	62	65
	Inversion [deg]	35	30	45	40
	Eversion [deg]	20	15	25	25

Subtalus	Inversion [deg]	26	21	35	25
	Eversion [deg]	10	11	8	9
		0 deg		30 deg	
Knee	Varus Test	-	-	-	-
	Valgus Test	-	-	-	-
At Rest		Right		Left	
Ankle		11 deg inversion		9 deg inversion	
Knee		6 deg genu valgum		4 deg genu valgum	

Table 7. Results from the range of motion test.

The subject has less ROM in comparison to the normal average ROM provided by the American Academy of Orthopaedic Surgeons (AAOS). This is most likely due to the stiffness and flexibility of the muscles. Eleven and nine degrees of inversion at the ankle are higher than normal, but this is likely because of muscle tightness and not a deformity of the joint. Six and four degrees of genu valgum at the knee are within normal ranges, especially for females due to the width of the pelvis.

5.4 On-Ice Data Collection for Determination of Joint Angles

The average maximum joint angles of the hip and knee joints were calculated and are shown in Table 8. The joint motions that were not included or are marked as N/A indicates that those joint motions did not occur during the butterfly movements.

	Hip	Knee
R. Abduction [deg]	39.46 ± 4.66	10.96 ± 2.15
L. Abduction [deg]	23.72 ± 5.75	10.46 ± 2.44
R. Internal Rotation [deg]	23.67 ± 4.39	N/A
L. Internal Rotation [deg]	15.01 ± 3.68	4.30± 3.71
R. External Rotation [deg]	N/A	5.71 ± 1.60
L. External Rotation [deg]	N/A	10.57 ± 2.12
R. Flexion [deg]	70.10 ± 5.79	100.74 ± 2.97
L. Flexion [deg]	65.60 ± 5.67	102.14 ± 3.53

Table 8. Maximum joint angles of the hip and knee joints for one butterfly movement.

The comparison of the maximum joint angles and the ROM are shown in Figures 23-26. For the hip joint, the joint angles that exceeded or came close to the ROM were the abduction angles for both hips. For the knee joint, ROM tests for abduction/adduction and internal/external rotation were not done since there is no standard for such a test and these motions could lead to injury. The joint motions in those directions were solely caused by the dynamic instability of the joint itself. The joint angles for the hip and knee joints for one butterfly are shown in Appendix G. In Appendix G, the black line represents the start of the recovery phase.

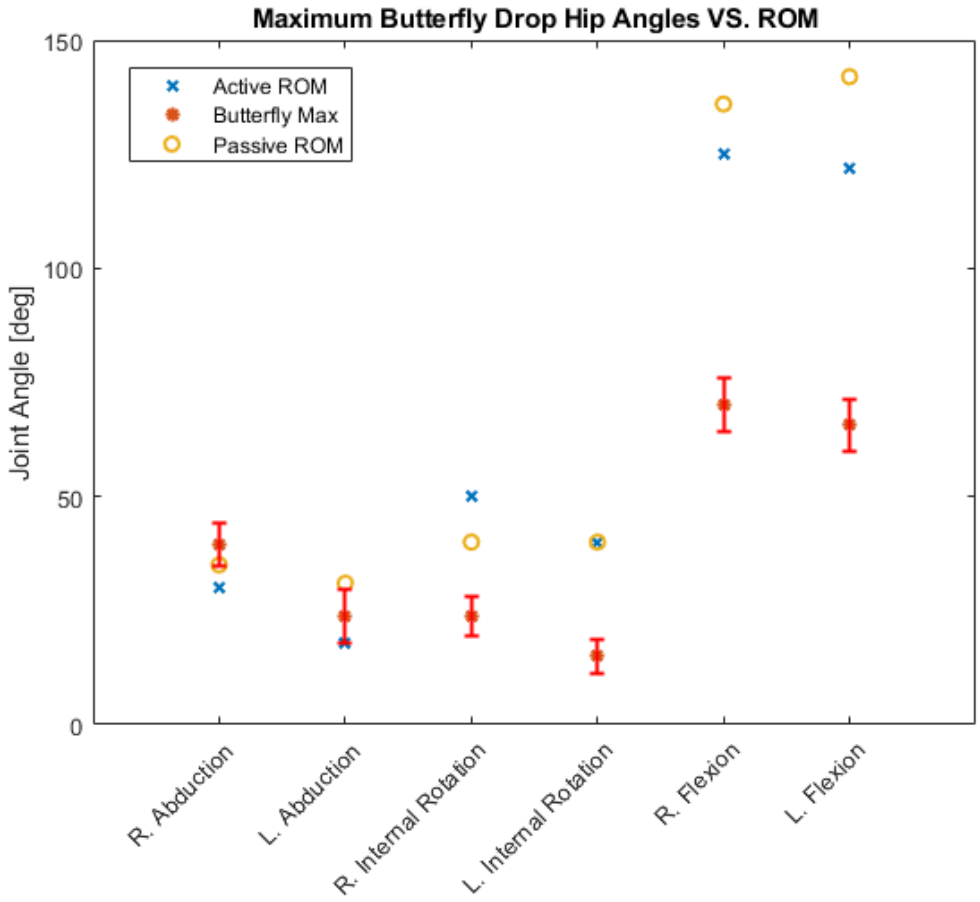

Figure 23. Comparison of maximum hip joint angles during one butterfly movement and the passive and active ROM.

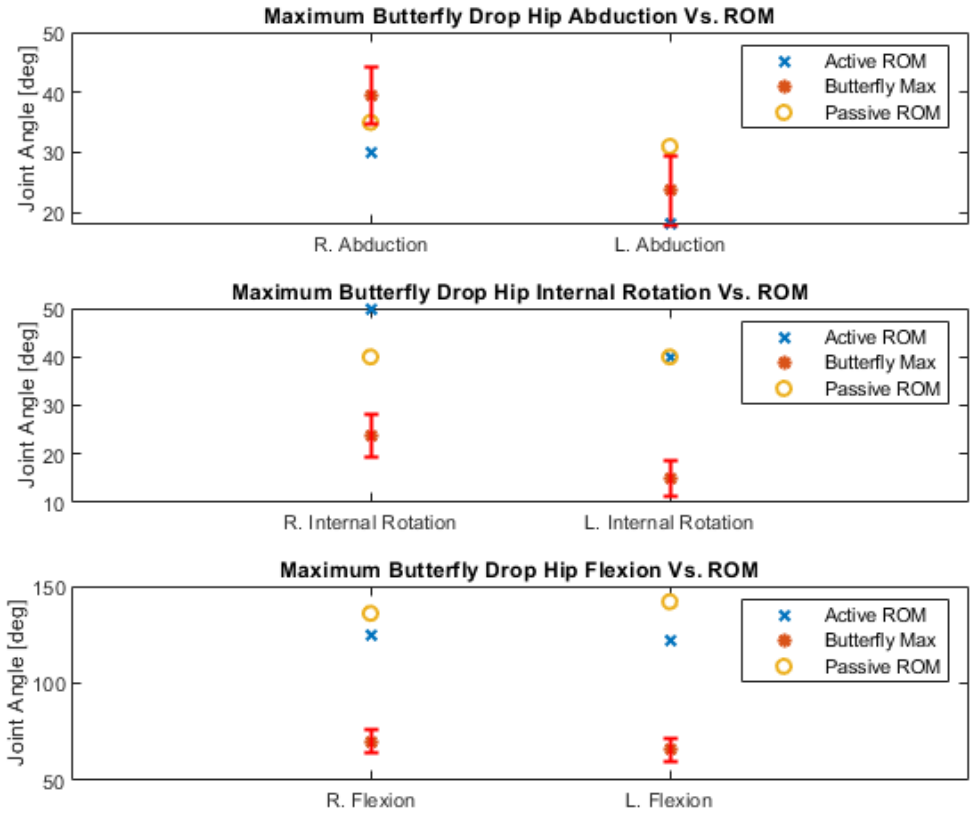

Figure 24. Comparison of the maximum hip joint angles of one butterfly movement and the passive and active ROM separated by joint motions for better scale.

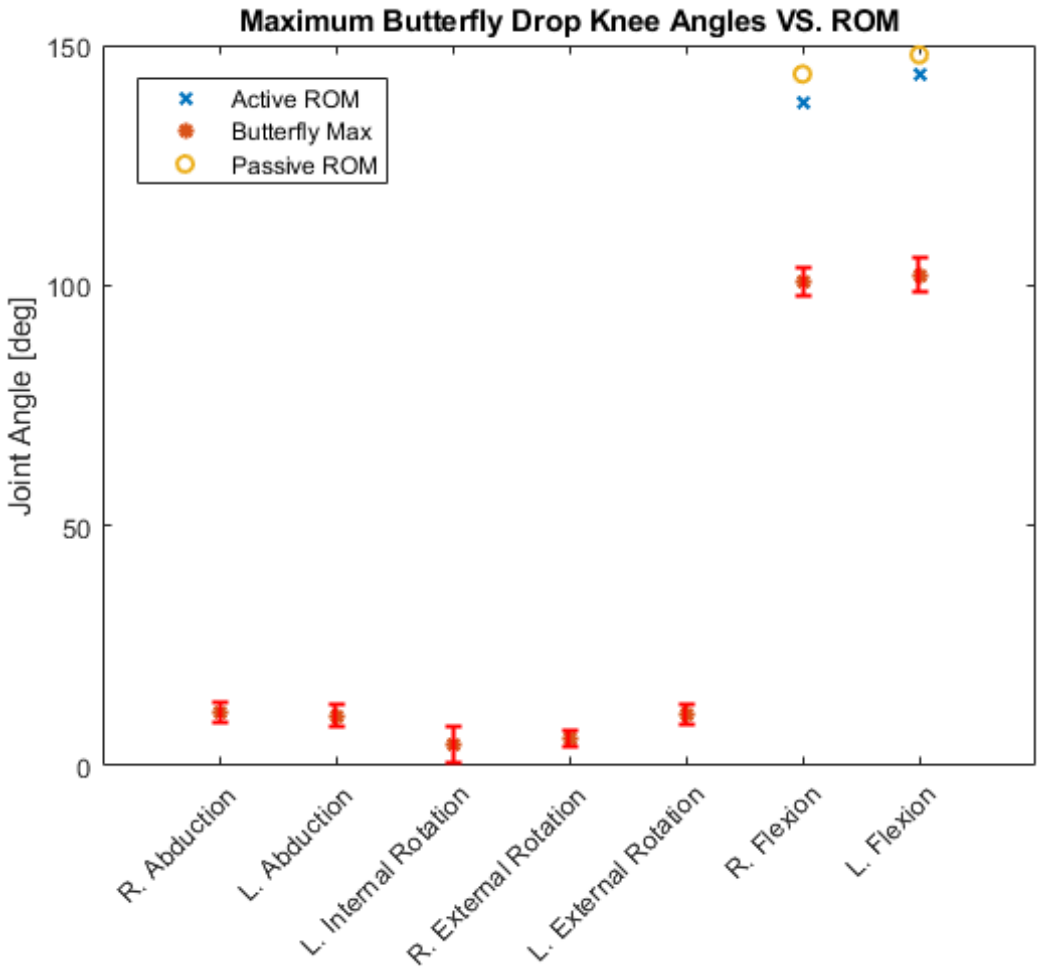

Figure 25. Comparison of the maximum knee joint angles for one butterfly movement and the passive and active ROM. The ROM test for knee abduction/adduction and internal/external rotation were not done, hence there is no data included in the plot.

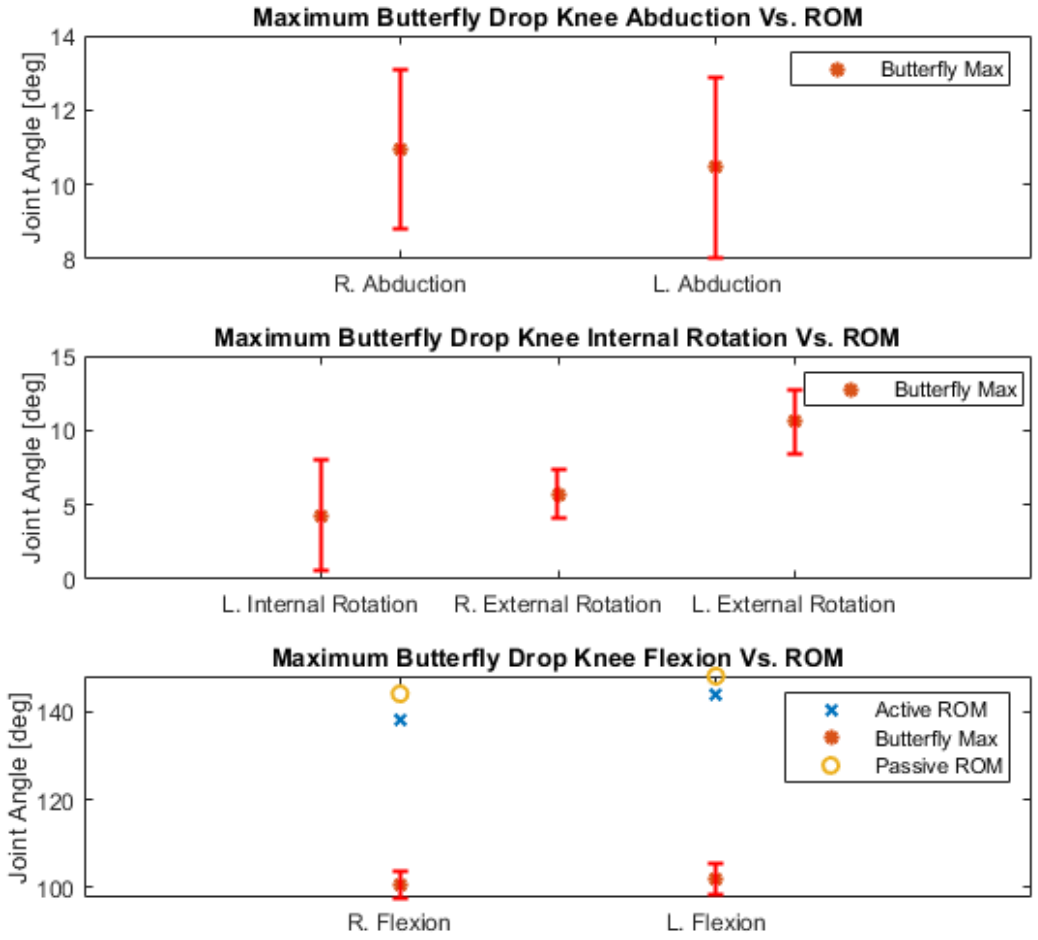

Figure 26. Comparison of the maximum knee joint angles for one butterfly movement and the passive and active ROM separated by joint motions for better scale. The ROM test for knee abduction/adduction and internal/external rotation were not done, hence there is no data included in the plot.

5.4 Results from the In-Lab Data Collection for the Inverse Dynamics Calculations

Data were collected from Xsens and force plates for inverse dynamic calculations to understand the loading of the joints during butterfly movements. All of the results from the inverse dynamic simulations use the local coordinate system from the individual joints. The .mvnx files obtained from the Xsens system have pre-defined segments in the file, which auto generate local coordinates at the individual joints. These local coordinate systems from the .mvnx files are defined differently than the local coordinate systems generated by V3D from a .c3d file. The representation of the Xsens local coordinate system in V3D and the local coordinate system generated by V3D from a .c3d file are shown in Figure 27.

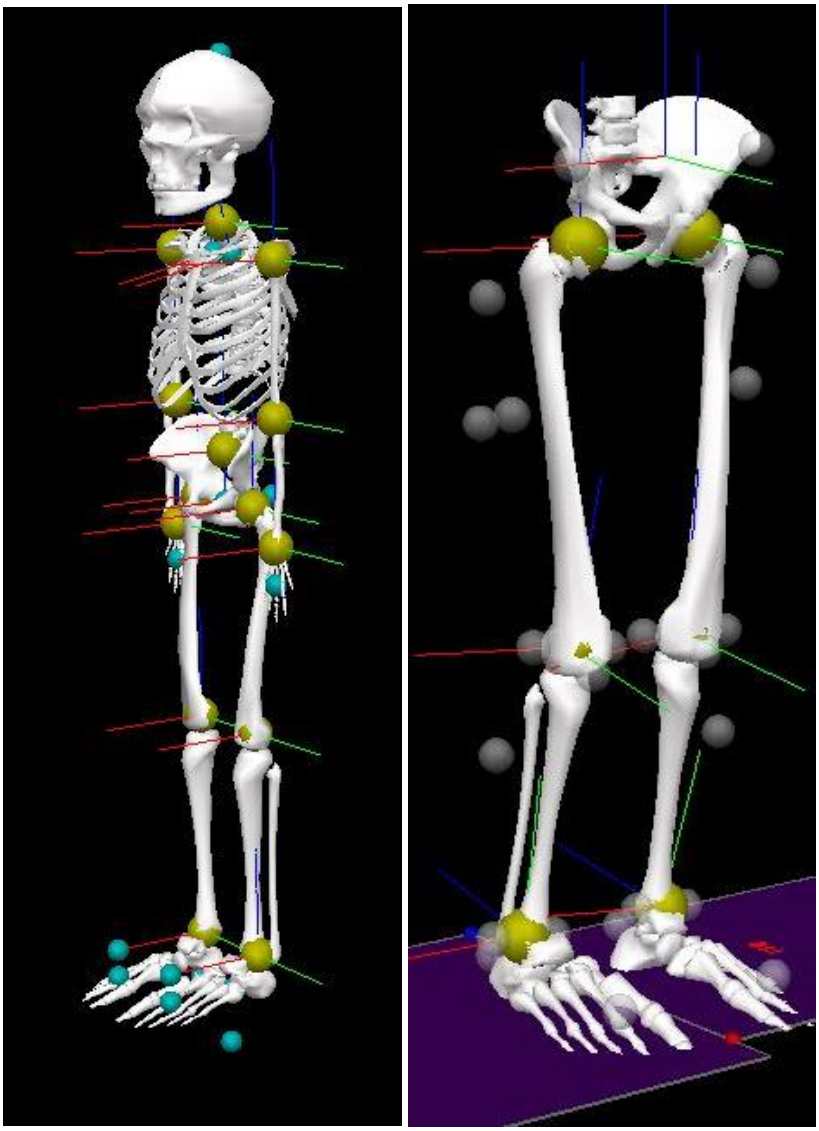

Figure 27. Xsens local coordinate definition in V3D (Left) and V3D local coordinate definition from c3d (Right) with red denoting the x-axis, green denoting the y-axis, and blue denoting the z-axis.

The maximum loads obtained are shown in Tables 9 and 10 and are based on the Xsens local coordinate system in V3D, as shown on the left of Figure 27. For example, a positive joint reaction force at the knee indicates that a force going in the forward direction is applied to the tibia. All of the loads are from the right legs since the single leg squat was performed using the right leg. Using normal walking as the base line, the percent difference in magnitude for the joint reaction forces, JRF, and joint reaction moments, JRM, were calculated for both single leg squat and butterfly movements. The results showed that there are about 40% to 70% percent increase in hip JRF magnitudes in the x and y directions respectively for butterfly motion comparing to those of normal walking. The magnitudes of knee JRF increase significantly in both X and Y directions for

butterfly motion in comparison to those for normal walking. The knee JRFs in the X and Y directions are potentially significant and could increase the potential for knee joint injuries since the joint structure was meant to bear weight only in the Z direction, the vertical direction, and not in the other directions. The magnitude of both the hip and knee JRM are at least 10 times greater than those of normal walking in both the X and Z directions.

	Hip JRF			Knee JRF		
	X	Y	Z	X	Y	Z
Normal Walking [N]	-148.22	-76.63	-535.95	-148.22	-76.63	-578.51
Single Leg Squat [N]	-211.50	-62.38	-463.26	-211.50	-62.38	-512.50
Butterfly [N]	-140.15	129.57	-404.41	-140.15	129.57	-384.20

Table 9. Hip and knee joint reaction forces for the butterfly motion, normal walking, and single leg squats.

	Hip JRM			Knee JRM		
	X	Y	Z	X	Y	Z
Normal Walking [Nm]	-38.90	34.78	6.19	22.35	23.44	-5.18
Single Leg Squat [Nm]	-42.52	46.43	12.07	-14.08	-65.75	-6.53
Butterfly [Nm]	437.33	-171.60	-163.25	381.07	-208.66	176.27

Table 10. Hip and knee joint reaction moments for the butterfly motion, normal walking, and single leg squats

6.0 Discussions

An Xsens MVN Awinda IMU motion capture system, was used in conjunction with AMTI force plates to quantify factors for potential injury such as joint angles and loads on the joints during butterfly motions. The methods and results were separated into two on-ice and in-lab portions. One focuses on the kinematics of the motion, more specifically the joint angles, and the other one focuses on the kinetics of the motion, to determine the JRF and JRM.

The kinematic results described in Section 5.4 suggest that the motions that the hip and knee joints were experiencing were internal hip rotation and abduction, and external rotation, flexion, and abduction of the knee. All of the motions, except for hip abduction, contribute to DKV. However, looking at Figure 28 shown below, during the dropping motion, the hips were actually adducting even when the joint angles were undergoing abduction. The joint motions at the knee and hip joints suggested that butterfly movement is a form of DKV as expected.

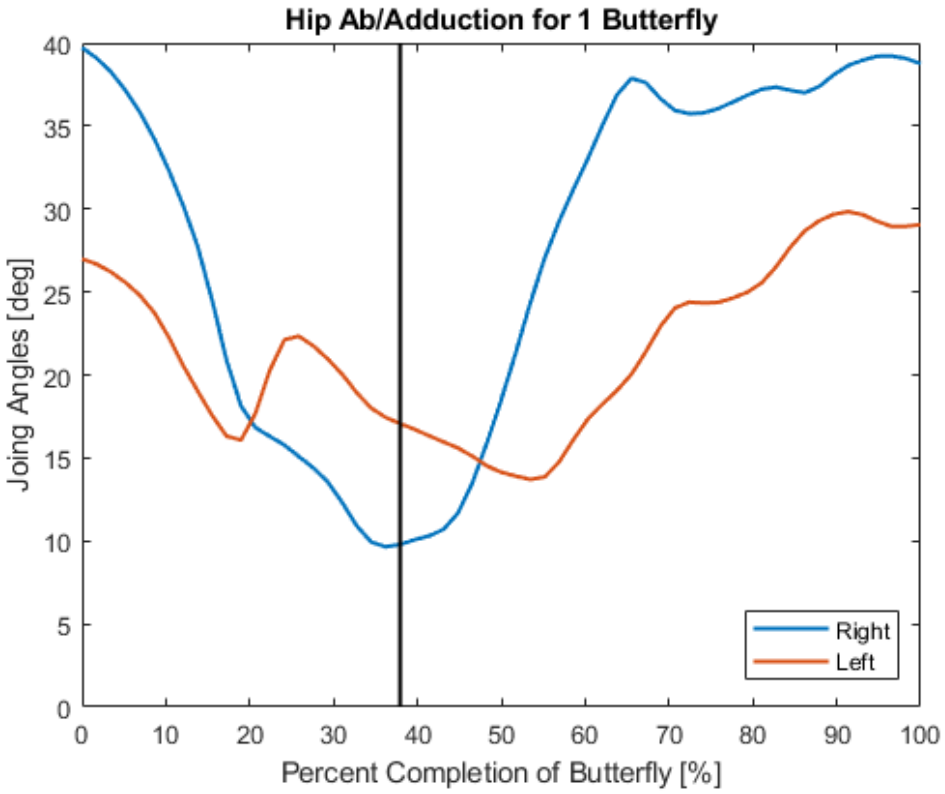

Figure 28. Hip abduction/adduction joint angle for one butterfly. The black line going vertically indicates the start of the recovery process. Positive direction is abduction and negative is adduction.

FAI is an injury that is more prevalent in athletes. The repeated motions of hip flexion and internal rotation or end-range motion in three planes could lead to cam-type

impingement, which is commonly seen in goalies [11, 23]. Based on the results shown in Figures 23 and 24, hip abduction is the only end-range motion that occurs during the dropping phase of a butterfly motion. Whiteside et al. concluded that the highest magnitude of joint angles were not observed during butterfly movements, but instead occurred during skating movements[11]. For the knee joint, the only joint motion that can be compared to the ROM is flexion. Not a lot of information can be obtained from Figures 25 and 26 since the ROM test cannot be done in abduction/adduction and internal/external rotation. The single leg squat test done by K. J. Pantano et al. showed that the knee valgus angles are within 15 – 25 degrees [24]. The maximum joint angles noticed in the butterfly movements for this study are less than the joint angles seen in single leg squats [24]. This indicates that the knee injuries among goalies are likely not caused solely by the joint angles during butterfly movement, but most likely the combination of the joint motions and the loads that the joint is experiencing.

The results shown in Table 9 suggest that that the hip JRF for butterfly motions are similar to those obtained during single leg squats, except for in the Y-direction which is more than two times the magnitude and is in the medial/lateral direction. In contrast, the knee JRF is much greater for the butterfly movements in both the X and Y directions. During single leg squats and walking motions, the majority of the force should be in the vertical direction since the motion occurs in the vertical direction and the structure of the human body is intended to bear weight in that direction. During butterfly movements, the lower leg bends laterally by almost 90 degrees. The knee joint is not bearing most of the vertical force under this type of motion. Hence, a much lower JRF in the Z-direction is observed. For the JRM results shown in Table 10, both the hip and knee JRM are higher for the butterfly motions than those obtained during single leg squats by at least three times the magnitude. However, DKV occurs during a single leg squat and is a task that researchers generally choose for DKV studies. Single leg squats are generally considered as minimal risk movements and are generally not harmful to research subjects. The results from this thesis suggest that the magnitudes of the JRM for single leg squats are all within two times the magnitudes of JRM for normal walking. The JRM for butterfly motions on the other hand are at least 4 times the magnitude of JRM for normal walking and could lead to different knee injuries.

The JRF and JRM obtained through inverse dynamic for normal walking and single leg squats were all based on single leg support whereas the butterfly motion was based on double leg support. For butterfly motion, each leg was supporting half of the body weight. Although the supported weight on the leg for the butterfly motion was only half the weight typically associated with normal walking and single leg squats, the JRF and JRM for the butterfly motion were still significantly larger than those associated with normal walking and single leg squats. ACL and MCL tears are the most commonly seen knee injuries among goalies. The JRM in the knee was determined to be 381 Nm in the X-direction and indicates that the MCL is under tension with a high applied load. The

ACL helps stabilize the knee during internal rotations and prevents the tibia from going forward. For the tibia, a rotational JRM of 176 Nm was obtained in the internal rotation direction and a 308 N JRF was obtained in the forward direction. Since the ACL is the main stabilizer for these motions, the results from the study suggest that the ACL under an extremely high stress during the butterfly motions.

The results from this thesis suggest that hip injuries among hockey goalies are likely caused by the ranges of motion that occur during butterfly motions. However, this is not the case for the knee joint. The knee joint angles during the butterfly motions were within acceptable ranges, but the loads on the knee joint during butterfly motions were extremely high.

Validation of the Xsens system was done by Zhang et al [25]. Zhang et al. compared joint angles during normal walking obtained from the Xsens system to an optical marker-based system[25]. Results showed excellent correlations between the two system for knee flexion/extension, hip flexion/extension, and internal/external rotation. For knee abduction/adduction and internal/external rotation, the results showed a 0.71 and a 0.88 coefficient of correlation (CMC) which are still considered as good correlations. For abduction/adduction at the hip, the results showed low correlation with a 0.39 CMC value [25]. The Xsens tends to capture higher joint angle for hip abduction/adduction and could possibly explain the abduction angle obtained in this study that exceeded the passive ROM on the right side.

Random uncertainties were calculated for the maximum joint angles during the dropping phase of the butterfly motion. For the hip joint, 0.7144, 0.5706, and 0.7225 degrees of random uncertainty were calculated for abduction, internal rotation, and flexion, respectively. For the knee joint, 0.3129, 0.4594, and 0.1948 degrees of random uncertainty were calculated for abduction, flexion, and external rotation, respectively. The joint angles obtained during butterfly motions for five trials are also shown in Appendix H and allow for qualitative comparison of the random uncertainty in the system. The random uncertainties showed how much variation was in the joint angle results for the on-ice data collection. Overall, the random uncertainties were small, and the results have no significant variation.

In addition to the inherent uncertainties associated with the motion capture hardware, there were a few potential sources of error that were introduced to the study. One of the biggest sources of errors was due to the placement of the lower leg Xsens sensors. By putting the sensors on the lateral side of the legs, up to 5 degrees of uncertainty could have been introduced into the joint angle measurements during certain joint motions. There was also a noticeable drift associate with the Xsens that was observed during the inverse dynamics test. After the global origin had been set, the origin moved to different locations between captures. A noticeable change in the subject's location in the V3D simulations, as shown in Figures 29, was seen. As a result,

the decision was made to redefine the origin between each capture and only have one trial per capture for the inverse dynamics analysis to ensure that the force was applied to a more precise location. The Xsens system sets the origin of the global coordinate system at the back of the right heel. Finding this location relies on the segment measurement inputs and how the algorithm calculates the location from the foot sensor. The location for the origin cannot be determined in the lab space. This error although small does exist.

The Xsens system relies on the calibration process and sensor placements to define a skeleton. When defining the skeleton, it assumes that all joints are at 0 degrees from the anatomical axis. The system is not able to identify any deformity that the participant has at rest. The subject for this study has 6 and 4 degrees of genu valgum at the right and left knees, respectively, at rest. However, the Xsens system assumes that there is 0 degrees of deviation from the anatomic axis. These angles, although small, can cause variations in the joint angle results. The joint angles for knee abduction/adduction should be higher than the ones measured. Some errors were also introduced during data processing operations, such as resampling. Any movement or slipping of the Xsens sensor could also result in errors in the study.

The inverse dynamic portion of the data collection was done in the lab due to the portability of the lab equipment. This portion of the test was also done wearing shoes instead of skates. In comparison to the environment for a real game situation, in which the skates are on ice, there will be more friction between the shoes and the lab floor. The JRF and JRM reported in this study is overestimated because the additional friction would increase the forces and moments input from the ground reaction.

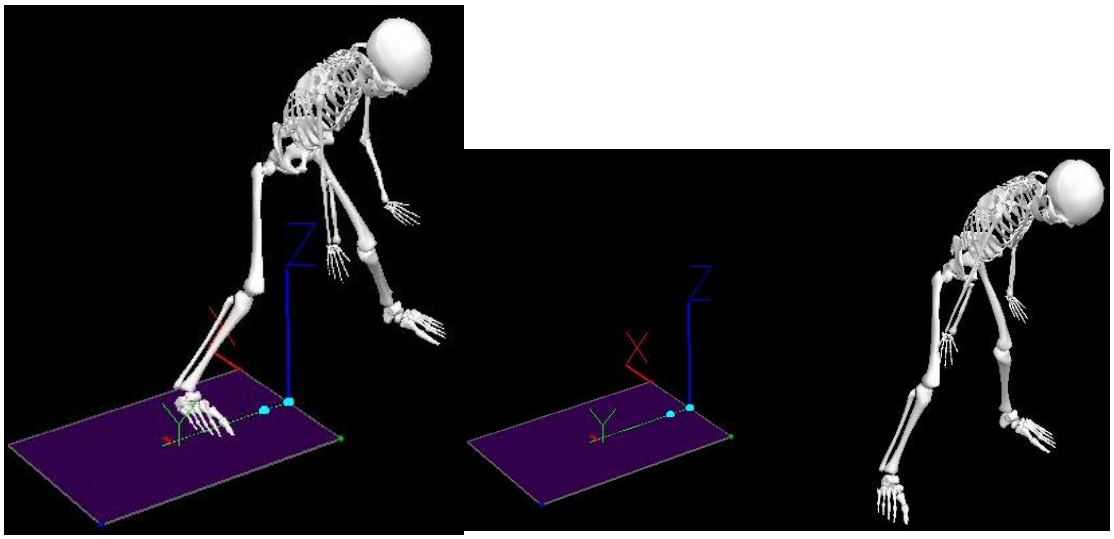

Figure 29. Position of the participant in the V3D simulation for the first butterfly (Left) and the fifth butterfly (Right)

No lateral movement was involved in this study and butterfly movements were the only motions that were studied. However, there are many more motions than just the butterfly movements for goaltending. In real game situations, there would be more lateral and dynamic movements involved. A current limitation of the Xsens is that the system cannot capture translational motion. Although future studies should focus on more types of movements involving goalies and more game-like situations, the technology may not currently permit these types of studies. A more in-depth look at how loads affect the ligaments and how close to failure the ligaments are during the butterfly motions would also be helpful in understanding the potential for injury going forward. Overall, the goal to quantify joint angles, JRF, and JRM at the knee and hip joints were achieved. The awkward joint motions of the butterfly movement, combined with the JRF going in the forward and lateral directions, and the JRM around the frontal and vertical axes were identified as factors that could increase the possibility of ACL and MCL tears.

7.0 Conclusions and Future Work

Several factors that could be associated with the potential for injuries during butterfly movements were identified through the findings of this thesis. Injuries at the knee joint are most likely not caused by the joint angles during butterfly movements. The most common knee injuries among hockey goalies, ACL and MCL tears, are potentially caused by the abnormally high JRF in the forward and lateral direction and the JRM that rotates around the frontal and vertical axes. Future work should focus on performing these tests in a game-like situation with more subjects. A more in-depth study should also be done with additional lab equipment such as electromyography (EMG) to obtain more information on muscle activation to further isolate the applied forces on ligaments. Further simulations should be done to simulate shear and transverse force in the joint to determine what are the acceptable loads at the joints and to further establish the relationships between different injuries and butterfly motions. An additional study focused on quantification of the uncertainties within the system should also be performed.

8.0 References

[1] How, H., 2012, 2012 Nhl Stanley Cup Final - Gam Six (Jonathan Quick), 12/12, http://www.zimbio.com/pictures/JibUdh0NtZC/2012+NHL+Stanley+Cup+Final+Gam%20e+Six/BgKiyvw8Umv/Jonathan+Quick
[2] Vollman, R., 2017, Nhl Goalies 2016-17, 5/22, http://www.hockeyabstract.com/testimonials/nhlgoalies2016-17
[3] Ross, J. R., Bedi, A., Stone, R. M., Sibilsky Enselman, E., Kelly, B. T., and Larson, C. M., 2015, "Characterization of Symptomatic Hip Impingement in Butterfly Ice Hockey Goalies," Arthroscopy, 31(4), pp. 635-42.
[4] Martini, F., 2015, Visual Anatomy & Physiology.
[5] "Average Ranges of Motion," American Academy of Orthopaedic Surgeons.
[6] Gwynne, C. R., and Curran, S. A., 2014, "Quantifying Frontal Plane Knee Motion During Single Limb Squats: Reliability and Validity of 2-Dimensional Measures," Int J Sports Phys Ther, 9(7), pp. 898-906.
[7] Powers, C. M., 2010, "The Influence of Abnormal Hip Mechanics on Knee Injury: A Biomechanical Perspective," J Orthop Sports Phys Ther, 40(2), pp. 42-51.
[8] Barrios, J. A., Heitkamp, C. A., Smith, B. P., Sturgeon, M. M., Suckow, D. W., and Sutton, C. R., 2016, "Three-Dimensional Hip and Knee Kinematics During Walking, Running, and Single-Limb Drop Landing in Females with and without Genu Valgum," Clin Biomech (Bristol, Avon), 31(pp. 7-11.
[9] Olson, M. D. S. A., Guilak, P. F., and Springerlink (Online Service), "Post-Traumatic Arthritis

Pathogenesis, Diagnosis and Management."
[10] Macintyre, K., Gomes, B., Mackenzie, S., and D'angelo, K., 2015, "Conservative Management of an Elite Ice Hockey Goaltender with Femoroacetabular Impingement (Fai): A Case Report," J Can Chiropr Assoc, 59(4), pp. 398-409.
[11] Whiteside, D., Deneweth, J. M., Bedi, A., Zernicke, R. F., and Goulet, G. C., 2015, "Femoroacetabular Impingement in Elite Ice Hockey Goaltenders: Etiological Implications of on-Ice Hip Mechanics," Am J Sports Med, 43(7), pp. 1689-97.
[12] Ferreira, D., 2016, Femoral Acetabular Impingement (Fai), 12/12, http://blog.zamst.us/femoral-acetabular-impingement-fai/
[13] Amanatullah, D., Antkowiak, T., Pillay, K., Patel, J., Refaat, M., A Toupadakis, C., and Amir, A., 2015, Femoroacetabular Impingement: Current Concepts in Diagnosis and Treatment.
[14] Reynolds, R. J., Walker, P. S., and Buza, J., 2017, "Mechanisms of Anterior-Posterior Stability of the Knee Joint under Load-Bearing," Journal of Biomechanics, 57(pp. 39-45.
[15] Agel, J., Arendt, E. A., and Bershadsky, B., 2005, "Anterior Cruciate Ligament Injury in National Collegiate Athletic Association Basketball and Soccer: A 13-Year Review," Am J Sports Med, 33(4), pp. 524-30.
[16] Hewett, T. E., Myer, G. D., Ford, K. R., Heidt, R. S., Colosimo, A. J., Mclean, S. G., Van Den Bogert, A. J., Paterno, M. V., and Succop, P., 2005, "Biomechanical Measures of Neuromuscular Control and Valgus Loading of the Knee Predict Anterior Cruciate Ligament Injury Risk in Female Athletes: A Prospective Study," Am J Sports Med, 33(4), pp. 492-501.
[17] Su, W. R., Chen, H. H., and Luo, Z. P., 2008, "Effect of Cyclic Stretching on the Tensile Properties of Patellar Tendon and Medial Collateral Ligament in Rat," Clin Biomech (Bristol, Avon), 23(7), pp. 911-7.
[18] Bizzini, M., Gorelick, M., and Drobny, T., 2006, "Lateral Meniscus Repair in a Professional Ice Hockey Goaltender: A Case Report with a 5-Year Follow-Up," Journal of Orthopaedic & Sports Physical Therapy, 36(2), pp. 89-100.

[19] Hoffman, M., Picture of the Knee, 12/12, https://www.webmd.com/pain-management/knee-pain/picture-of-the-knee#1
[20] Wolfgang, T., "Biomechanical Quantification of the Dynamic Knee

Valgus Using Inertial Sensor System Myomotion®," Master of Science in Biomechanics Motor Motion Analysis Justus Liebig University Giessen/The Mittelhessen University of Applied Science.
[21] Roetenberg, D., Luinge, H., and Slycke, P. J., 2013, "Xsens Mvn : Full 6 Dof Human Motion Tracking Using Miniature Inertial Sensors."
[22] Wijdicks, C. A., Philippon, M. J., Civitarese, D. M., and Laprade, R. F., 2014, "A Mandated Change in Goalie Pad Width Has No Effect on Ice Hockey Goaltender Hip Kinematics," Clin J Sport Med, 24(5), pp. 403-8.
[23] Mar©*N-Pe©*a, L., 2012, "Femoroacetabular Impingement," Springer,, Berlin ; New York.
[24] Pantano, K. J., White, S. C., Gilchrist, L. A., and Leddy, J., 2005, "Differences in Peak Knee Valgus Angles between Individuals with High and Low Q-Angles During a Single Limb Squat," Clin Biomech (Bristol, Avon), 20(9), pp. 966-72.
[25] Jun-Tian Zhang and Alison, C. N. A. B. B. A. Q. L., 2013, "Concurrent Validation of Xsens Mvn Measurement of Lower Limb Joint Angular Kinematics," Physiological Measurement, 34(8), pp. N63.

Appendix

A. MATLAB Script for MVNX Data Processing

```
%% Thesis Xsens Analysis
% Tzu-Ting (Tiffany) Hsu
clear all
close all
clc

%% Load XVMN Data
% load data
tree = load_mvnx('S1-10-Non Stop_1');
% tree = load_mvnx('S1-10-Non Stop_2');
% tree = load_mvnx('S1-10-Non Stop_3');
% read some basic data from the file
mvnxVersion = tree;
fileComments = tree.subject.comment;
%read some basic properties of the subject;
frameRate = tree.subject.frameRate;
suitLabel = tree.subject.label;
originalFilename = tree.subject.originalFilename;
recDate = tree.subject.recDate;
segmentCount = tree.subject.segmentCount;
%retrieve sensor labels
%creates a struct with sensor data
if isfield(tree.subject,'sensors') && isstruct(tree.subject.sensors)
    sensorData = tree.subject.sensors.sensor;
end
%retrieve segment labels
%creates a struct with segment definitions
if isfield(tree.subject,'segments') && isstruct(tree.subject.segments)
    segmentData = tree.subject.segments.segment;
end

%creates a struct with joint definitionsJ_A.jRightHip(D_S(i):R_S(i),j)
if isfield(tree.subject,'joints') && isstruct(tree.subject.joints)
    jointData = tree.subject.joints.joint;
end

%% Seperation of Joint Angle
J_name = {jointData.label};
for i = 1:length(tree.subject.frames.frame)-3
    for j = 1:length(jointData)
        for k = 1:3
            J_A.(J_name{j})(i,k) =
tree.subject.frames.frame(i+3).jointAngle(3*(j-1)+k);
        end
    end
end

%% Finding Max of Motion
V_end = 733; % For S1 10 Non Stop 1
% V_end = 800; % For S1 10 Non Stop 2
% V_end = 690; % For S1 10 Non Stop 3

% Take out data points before and after the actual butterfly test for S1 10 Non
Stop 1
% J_A.jRightHip(1:125,:) = 0;
% J_A.jRightHip(V_end:end,:) = 0;
% J_A.jRightKnee(1:125,:) = 0;
% J_A.jRightKnee(V_end:end,:) = 0;
```

```
% Take out data points before and after the actual butterfly test for S1 10 Non
Stop 2
% J_A.jRightHip(1:150,:) = 0;
% J_A.jRightHip(V_end:end,:) = 0;
% J_A.jRightKnee(1:150,:) = 0;
% J_A.jRightKnee(V_end:end,:) = 0;

% Take out data points before and after the actual butterfly test for S1 10 Non
Stop 3
% J_A.jRightHip(1:133,:) = 0;
% J_A.jRightHip(V_end:end,:) = 0;
% J_A.jRightKnee(1:133,:) = 0;
% J_A.jRightKnee(V_end:end,:) = 0;

% figure;
% plot(movmean(J_A.jRightHip(:,3),5))
% hold on
% plot(movmean(J_A.jLeftHip(:,3),5))
%
% figure;
% plot(movmean(J_A.jRightHip(:,1),5))
% hold on
% plot(movmean(J_A.jLeftHip(:,1),5))

[pks, D_S]= findpeaks(movmean(J_A.jRightHip(:,3),5),'MinPeakHeight', 55,
'MinPeakWidth', 10);

[pks, R_S]= findpeaks(-movmean(J_A.jRightHip(:,1),5),'MinPeakHeight', -17,
'MinPeakWidth', 12);


%% Max Dropping Angle Calculation
for i = 1:length(D_S)
    for j = 1:3
        Max.Drop.RHip(i,j) =  max(J_A.jRightHip(D_S(i):R_S(i),j));
        Max.Drop.RKnee(i,j) =  max(J_A.jRightKnee(D_S(i):R_S(i),j));
        Max.Drop.RAnkle(i,j) =  max(J_A.jRightAnkle(D_S(i):R_S(i),j));
        Min.Drop.RHip(i,j) =  min(J_A.jRightHip(D_S(i):R_S(i),j));
        Min.Drop.RKnee(i,j) =  min(J_A.jRightKnee(D_S(i):R_S(i),j));
        Min.Drop.RAnkle(i,j) =  min(J_A.jRightAnkle(D_S(i):R_S(i),j));
        Max.Drop.LHip(i,j) =  max(J_A.jLeftHip(D_S(i):R_S(i),j));
        Max.Drop.LKnee(i,j) =  max(J_A.jLeftKnee(D_S(i):R_S(i),j));
        Max.Drop.LAnkle(i,j) =  max(J_A.jLeftAnkle(D_S(i):R_S(i),j));
        Min.Drop.LHip(i,j) =  min(J_A.jLeftHip(D_S(i):R_S(i),j));
        Min.Drop.LKnee(i,j) =  min(J_A.jLeftKnee(D_S(i):R_S(i),j));
        Min.Drop.LAnkle(i,j) =  min(J_A.jLeftAnkle(D_S(i):R_S(i),j));

    end

end

%% Max Recovery Angle Calculation
for i = 1: length(D_S)
    for j = 1:3
        if i <10
            Max.Recover.RHip(i,j) =  max(J_A.jRightHip(R_S(i):D_S(i+1),j));
            Max.Recover.RKnee(i,j) =  max(J_A.jRightKnee(R_S(i):D_S(i+1),j));
            Max.Recover.RAnkle(i,j) =  max(J_A.jRightAnkle(R_S(i):D_S(i+1),j));
            Min.Recover.RHip(i,j) =  min(J_A.jRightHip(R_S(i):D_S(i+1),j));
            Min.Recover.RKnee(i,j) =  min(J_A.jRightKnee(R_S(i):D_S(i+1),j));
```

```
            Min.Recover.RAnkle(i,j) =  min(J_A.jRightAnkle(R_S(i):D_S(i+1),j));
            Max.Recover.LHip(i,j) =  max(J_A.jLeftHip(R_S(i):D_S(i+1),j));
            Max.Recover.LKnee(i,j) =  max(J_A.jLeftKnee(R_S(i):D_S(i+1),j));
            Max.Recover.LAnkle(i,j) =  max(J_A.jLeftAnkle(R_S(i):D_S(i+1),j));
            Min.Recover.LHip(i,j) =  min(J_A.jLeftHip(R_S(i):D_S(i+1),j));
            Min.Recover.LKnee(i,j) =  min(J_A.jLeftKnee(R_S(i):D_S(i+1),j));
            Min.Recover.LAnkle(i,j) =  min(J_A.jLeftAnkle(R_S(i):D_S(i+1),j));
        else
            Max.Recover.RHip(i,j) =  max(J_A.jRightHip(R_S(i):(V_end-1),j));
            Max.Recover.RKnee(i,j) =  max(J_A.jRightKnee(R_S(i):(V_end-1),j));
            Max.Recover.RAnkle(i,j) =   max(J_A.jRightAnkle(R_S(i):(V_end-1),j));
            Min.Recover.RHip(i,j) =  min(J_A.jRightHip(R_S(i):(V_end-1),j));
            Min.Recover.RKnee(i,j) =  min(J_A.jRightKnee(R_S(i):(V_end-1),j));
            Min.Recover.RAnkle(i,j) =   min(J_A.jRightAnkle(R_S(i):(V_end-1),j));
            Max.Recover.LHip(i,j) =  max(J_A.jLeftHip(R_S(i):(V_end-1),j));
            Max.Recover.LKnee(i,j) =  max(J_A.jLeftKnee(R_S(i):(V_end-1),j));
            Max.Recover.LAnkle(i,j) =  max(J_A.jLeftAnkle(R_S(i):(V_end-1),j));
            Min.Recover.LHip(i,j) =  min(J_A.jLeftHip(R_S(i):(V_end-1),j));
            Min.Recover.LKnee(i,j) =  min(J_A.jLeftKnee(R_S(i):(V_end-1),j));
            Min.Recover.LAnkle(i,j) =  min(J_A.jLeftAnkle(R_S(i):(V_end-1),j));
        end
    end
```

B. MATLAB Script for Joint Angle Data Processing

```
%% Final Joint Angle Comparisons
% Tzu-Ting (Tiffany) Hsu
clear all
close all
clc

%% Load Final Joint Angle Data and ROM Data
Drop.Max = dlmread('Final Joint Angles.txt', '\t', [3 1 32 16]); % Load drop
max (abduction, internal rotationt, flexion)
Drop.Min = dlmread('Final Joint Angles.txt', '\t', [36 1 65 16]); % Load drop
min (adduction, external rotationt, extension)
Recovery.Max = dlmread('Final Joint Angles Recovery.txt', '\t', [3 1 32 16]); %
Load recovery max (abduction, internal rotationt, flexion)
Recovery.Min = dlmread('Final Joint Angles Recovery.txt', '\t', [36 1 65 16]); %
Load recovery min (adduction, external rotationt, extension)
Active.Max = dlmread('ROM Results.txt', '\t', [3 8 3 23]); % Load active ROM
max (abduction, internal rotationt, flexion)
Active.Min = dlmread('ROM Results.txt', '\t', [5 8 5 23]); % Load active ROM
min (adduction, external rotationt, extension)
Passive.Max = dlmread('ROM Results.txt', '\t', [9 8 9 23]); % Load passive ROM
max (abduction, internal rotationt, flexion)
Passive.Min = dlmread('ROM Results.txt', '\t', [11 8 11 23]); % Load passive
ROM min (adduction, external rotationt, extension)

%% Apply Functions to Data
Drop = PRO(Drop);
Recovery = PRO(Recovery);
Active = ROM(Active);
Passive = ROM(Passive);

%% Grouping Data
y1 = Group(Drop, Active.Drop, Passive.Drop);
Drop.Hip.x = {'R. Abduction', 'L. Abduction', 'R. Internal Rotation', ...
    'L. Internal Rotation', 'R. Flexion', 'L. Flexion'};
Drop.Hip.y = [y1.y(1,:); y1.y(4,:); y1.y(2,:); y1.y(5,:); y1.y(3,:); y1.y(6,:)];
Drop.Hip.err = [y1.err(1), y1.err(4), y1.err(2), y1.err(5), y1.err(3),
y1.err(6)];

Drop.Knee.x = {'R. Abduction', 'L. Abduction', 'L. Internal Rotation', ...
    'R. External Rotation', 'L. External Rotation', 'R. Flexion', 'L. Flexion'};
Drop.Knee.y = [y1.y(7,:); y1.y(9:10,:); y1.y(16:17,:); y1.y(8,:); y1.y(11,:)];
Drop.Knee.err = [y1.err(7), y1.err(9:10), y1.err(16:17), y1.err(8), y1.err(11)];

Drop.Ankle.x = {'R. Eversion', 'L. Eversion', 'R. Inversion', ...
    'L. Inversion', 'R. Dorsiflexion', 'L. Dorsiflexion'};
Drop.Ankle.y = [y1.y(12,:); y1.y(14,:); y1.y(18:19,:); y1.y(13,:); y1.y(15,:);];
Drop.Ankle.err = [y1.err(12), y1.err(14), y1.err(18:19), y1.err(13),
y1.err(15)];

y2 = Group(Recovery, Active.Recovery, Passive.Recovery);
Recovery.Hip.x = {'R. Abduction', 'L. Abduction', 'R. Internal Rotation', ...
    'L. Internal Rotation', 'R. External Rotation', 'R. Flexion', 'L. Flexion'};
Recovery.Hip.y = [y2.y(1,:); y2.y(4,:); y2.y(2,:); y2.y(5,:); y2.y(17,:);
y2.y(3,:); y2.y(6,:)];
Recovery.Hip.err = [y2.err(1), y2.err(4), y2.err(2), y2.err(5), y2.err(17),
y2.err(3), y2.err(6)];

Recovery.Knee.x = {'R. Abduction', 'L. Abduction', 'L. Adduction', ...
    'R. Internal Rotation', 'L. Internal Rotation', 'R. External Rotation', ...
    'L. External Rotation', 'R. Flexion', 'L. Flexion'};
```

```
Recovery.Knee.y = [y2.y(7,:); y2.y(10,:); y2.y(19,:); y2.y(8,:);
y2.y(11,:); ...
    y2.y(18,:);  y2.y(20,:);  y2.y(9,:);  y2.y(12,:)];
Recovery.Knee.err = [y2.err(7), y2.err(10), y2.err(19), y2.err(8),
y2.err(11), ...
    y2.err(18),  y2.err(20),  y2.err(9),  y2.err(12)];

Recovery.Ankle.x = {'R. Eversion', 'L. Eversion', 'R. Inversion', ...
    'L. Inversion', 'R. Dorsiflexion', 'L. Dorsiflexion'};
Recovery.Ankle.y = [y2.y(13,:); y2.y(15,:); y2.y(21:22,:); y2.y(14,:);
y2.y(16,:)];
Recovery.Ankle.err = [y2.err(13), y2.err(15), y2.err(21:22), y2.err(14),
y2.err(16)];

%% Plotting Dropping Hip
figure;
plot(1:length(Drop.Hip.y), Drop.Hip.y(:,1), 'x', 'LineWidth', 1.5)
hold on
plot(1:length(Drop.Hip.y), Drop.Hip.y(:,2), '*', 'LineWidth', 1.5)
hold on
plot(1:length(Drop.Hip.y), Drop.Hip.y(:,3), 'o', 'LineWidth', 1.5)
errorbar(Drop.Hip.y(:,2), Drop.Hip.err, 'r', 'LineStyle', 'none', 'LineWidth',
1.5)
title('Maximum Butterfly Drop Hip Angles VS. ROM')
legend('Active ROM', 'Butterfly Max', 'Passive ROM')
xlim([0 length(Drop.Hip.y) + 1])
xticks([1 2 3 4 5 6])
xticklabels(Drop.Hip.x)
xtickangle(45)
ylabel('Joint Angle [deg]')

figure;
subplot(3,1,1)
plot(1:2, Drop.Hip.y(1:2,1), 'x', 'LineWidth', 1.5)
hold on
plot(1:2, Drop.Hip.y(1:2,2), '*', 'LineWidth', 1.5)
hold on
plot(1:2, Drop.Hip.y(1:2,3), 'o', 'LineWidth', 1.5)
errorbar(Drop.Hip.y(1:2,2), Drop.Hip.err(1:2), 'r', 'LineStyle', 'none',
'LineWidth', 1.5)
title('Maximum Butterfly Drop Hip Abduction Vs. ROM')
legend('Active ROM', 'Butterfly Max', 'Passive ROM')
xlim([0 3])
xticks([1 2])
xticklabels([Drop.Hip.x{1}; Drop.Hip.x{2}])
ylabel('Joint Angle [deg]')

subplot(3,1,2)
plot(1:2, Drop.Hip.y(3:4,1), 'x', 'LineWidth', 1.5)
hold on
plot(1:2, Drop.Hip.y(3:4,2), '*', 'LineWidth', 1.5)
hold on
plot(1:2, Drop.Hip.y(3:4,3), 'o', 'LineWidth', 1.5)
errorbar(Drop.Hip.y(3:4,2), Drop.Hip.err(3:4), 'r', 'LineStyle', 'none',
'LineWidth', 1.5)
title('Maximum Butterfly Drop Hip Internal Rotation Vs. ROM')
legend('Active ROM', 'Butterfly Max', 'Passive ROM')
xlim([0 3])
xticks([1 2])
xticklabels([Drop.Hip.x{3}; Drop.Hip.x{4}])
ylabel('Joint Angle [deg]')
```

```
subplot(3,1,3)
plot(1:2, Drop.Hip.y(5:6,1), 'x', 'LineWidth', 1.5)
hold on
plot(1:2, Drop.Hip.y(5:6,2), '*', 'LineWidth', 1.5)
hold on
plot(1:2, Drop.Hip.y(5:6,3), 'o', 'LineWidth', 1.5)
errorbar(Drop.Hip.y(5:6,2), Drop.Hip.err(5:6), 'r', 'LineStyle', 'none',
'LineWidth', 1.5)
title('Maximum Butterfly Drop Hip Flexion Vs. ROM')
legend('Active ROM', 'Butterfly Max', 'Passive ROM')
xlim([0 3])
xticks([1 2])
xticklabels([Drop.Hip.x{5}; Drop.Hip.x{6}])
ylabel('Joint Angle [deg]')

%% Plotting Dropping Knee
figure;
plot(1:length(Drop.Knee.y), Drop.Knee.y(:,1), 'x', 'LineWidth', 1.5)
hold on
plot(1:length(Drop.Knee.y), Drop.Knee.y(:,2), '*', 'LineWidth', 1.5)
hold on
plot(1:length(Drop.Knee.y), Drop.Knee.y(:,3), 'o', 'LineWidth', 1.5)
errorbar(Drop.Knee.y(:,2), Drop.Knee.err, 'r', 'LineStyle', 'none', 'LineWidth',
1.5)
title('Maximum Butterfly Drop Knee Angles VS. ROM')
legend('Active ROM', 'Butterfly Max', 'Passive ROM')
xlim([0 length(Drop.Knee.y) + 1])
xticks([1 2 3 4 5 6 7])
xticklabels(Drop.Knee.x)
xtickangle(45)
ylabel('Joint Angle [deg]')

figure;
subplot(3,1,1)
plot(1:2, Drop.Knee.y(1:2,1), 'x', 'LineWidth', 1.5)
hold on
p1 = plot(1:2, Drop.Knee.y(1:2,2), '*', 'LineWidth', 1.5);
hold on
plot(1:2, Drop.Knee.y(1:2,3), 'o', 'LineWidth', 1.5)
errorbar(Drop.Knee.y(1:2,2), Drop.Knee.err(1:2), 'r', 'LineStyle', 'none',
'LineWidth', 1.5)
title('Maximum Butterfly Drop Knee Abduction Vs. ROM')
legend([p1], {'Butterfly Max'})
xlim([0 3])
xticks([1 2])
xticklabels([Drop.Knee.x{1}; Drop.Knee.x{2}])
ylabel('Joint Angle [deg]')

subplot(3,1,2)
plot(1:3, Drop.Knee.y(3:5,1), 'x', 'LineWidth', 1.5)
hold on
p1 = plot(1:3, Drop.Knee.y(3:5,2), '*', 'LineWidth', 1.5);
hold on
plot(1:3, Drop.Knee.y(3:5,3), 'o', 'LineWidth', 1.5)
errorbar(Drop.Knee.y(3:5,2), Drop.Knee.err(3:5), 'r', 'LineStyle', 'none',
'LineWidth', 1.5)
title('Maximum Butterfly Drop Knee Internal Rotation Vs. ROM')
legend([p1], {'Butterfly Max'})
xlim([0 4])
xticks([1 2 3])
xticklabels([Drop.Knee.x{3}; Drop.Knee.x{4}; Drop.Knee.x{5}])
ylabel('Joint Angle [deg]')
```

```
subplot(3,1,3)
plot(1:2, Drop.Knee.y(6:7,1), 'x', 'LineWidth', 1.5)
hold on
plot(1:2, Drop.Knee.y(6:7,2), '*', 'LineWidth', 1.5)
hold on
plot(1:2, Drop.Knee.y(6:7,3), 'o', 'LineWidth', 1.5)
errorbar(Drop.Knee.y(6:7,2), Drop.Knee.err(6:7), 'r', 'LineStyle', 'none',
'LineWidth', 1.5)
title('Maximum Butterfly Drop Knee Flexion Vs. ROM')
legend('Active ROM', 'Butterfly Max', 'Passive ROM')
xlim([0 3])
xticks([1 2])
xticklabels([Drop.Knee.x{6}; Drop.Knee.x{7}])
ylabel('Joint Angle [deg]')

%% Plotting Recovery Hip
figure;
plot(1:length(Recovery.Hip.y), Recovery.Hip.y(:,1), 'x', 'LineWidth', 1.5)
hold on
plot(1:length(Recovery.Hip.y), Recovery.Hip.y(:,2), '*', 'LineWidth', 1.5)
hold on
plot(1:length(Recovery.Hip.y), Recovery.Hip.y(:,3), 'o', 'LineWidth', 1.5)
errorbar(Recovery.Hip.y(:,2), Recovery.Hip.err, 'r', 'LineStyle', 'none',
'LineWidth', 1.5)
title('Maximum Butterfly Recovery Hip Angles VS. ROM')
legend('Active ROM', 'Butterfly Max', 'Passive ROM')
xlim([0 length(Recovery.Hip.y) + 1])
xticks([1 2 3 4 5 6 7])
xticklabels(Recovery.Hip.x)
xtickangle(45)
ylabel('Joint Angle [deg]')

figure;
subplot(3,1,1)
plot(1:2, Recovery.Hip.y(1:2,1), 'x', 'LineWidth', 1.5)
hold on
plot(1:2, Recovery.Hip.y(1:2,2), '*', 'LineWidth', 1.5)
hold on
plot(1:2, Recovery.Hip.y(1:2,3), 'o', 'LineWidth', 1.5)
errorbar(Recovery.Hip.y(1:2,2), Recovery.Hip.err(1:2), 'r', 'LineStyle', 'none',
'LineWidth', 1.5)
title('Maximum Butterfly Recovery Hip Abduction Vs. ROM')
legend('Active ROM', 'Butterfly Max', 'Passive ROM')
xlim([0 3])
xticks([1 2])
xticklabels([Recovery.Hip.x{1}; Recovery.Hip.x{2}])
ylabel('Joint Angle [deg]')

subplot(3,1,2)
plot(1:3, Recovery.Hip.y(3:5,1), 'x', 'LineWidth', 1.5)
hold on
plot(1:3, Recovery.Hip.y(3:5,2), '*', 'LineWidth', 1.5)
hold on
plot(1:3, Recovery.Hip.y(3:5,3), 'o', 'LineWidth', 1.5)
errorbar(Recovery.Hip.y(3:5,2), Recovery.Hip.err(3:5), 'r', 'LineStyle', 'none',
'LineWidth', 1.5)
title('Maximum Butterfly Recovery Hip Internal Rotation Vs. ROM')
legend('Active ROM', 'Butterfly Max', 'Passive ROM')
xlim([0 4])
xticks([1 2 3])
xticklabels([Recovery.Hip.x{3}; Recovery.Hip.x{4}; Recovery.Hip.x{5}])
```

```
ylabel('Joint Angle [deg]')

subplot(3,1,3)
plot(1:2, Recovery.Hip.y(6:7,1), 'x', 'LineWidth', 1.5)
hold on
plot(1:2, Recovery.Hip.y(6:7,2), '*', 'LineWidth', 1.5)
hold on
plot(1:2, Recovery.Hip.y(6:7,3), 'o', 'LineWidth', 1.5)
errorbar(Recovery.Hip.y(6:7,2), Recovery.Hip.err(6:7), 'r', 'LineStyle', 'none',
'LineWidth', 1.5)
title('Maximum Butterfly Recovery Hip Flexion Vs. ROM')
legend('Active ROM', 'Butterfly Max', 'Passive ROM')
xlim([0 3])
xticks([1 2])
xticklabels([Recovery.Hip.x{6}; Recovery.Hip.x{7}])
ylabel('Joint Angle [deg]')

%% Plotting Recovery Knee
figure;
plot(1:length(Recovery.Knee.y), Recovery.Knee.y(:,1), 'x', 'LineWidth', 1.5)
hold on
plot(1:length(Recovery.Knee.y), Recovery.Knee.y(:,2), '*', 'LineWidth', 1.5)
hold on
plot(1:length(Recovery.Knee.y), Recovery.Knee.y(:,3), 'o', 'LineWidth', 1.5)
errorbar(Recovery.Knee.y(:,2), Recovery.Knee.err, 'r', 'LineStyle', 'none',
'LineWidth', 1.5)
title('Maximum Butterfly Recovery Knee Angles VS. ROM')
legend('Active ROM', 'Butterfly Max', 'Passive ROM')
xlim([0 length(Recovery.Knee.y) + 1])
xticks([1 2 3 4 5 6 7 8 9])
xticklabels(Recovery.Knee.x)
xtickangle(45)
ylabel('Joint Angle [deg]')

figure;
subplot(3,1,1)
plot(1:3, Recovery.Knee.y(1:3,1), 'x', 'LineWidth', 1.5)
hold on
plot(1:3, Recovery.Knee.y(1:3,2), '*', 'LineWidth', 1.5)
hold on
plot(1:3, Recovery.Knee.y(1:3,3), 'o', 'LineWidth', 1.5)
errorbar(Recovery.Knee.y(1:3,2), Recovery.Knee.err(1:3), 'r', 'LineStyle',
'none', 'LineWidth', 1.5)
title('Maximum Butterfly Recovery Knee Abduction Vs. ROM')
legend('Active ROM', 'Butterfly Max', 'Passive ROM')
xlim([0 4])
xticks([1 2 3])
xticklabels([Recovery.Knee.x{1}; Recovery.Knee.x{2}; Recovery.Knee.x{3}])
ylabel('Joint Angle [deg]')

subplot(3,1,2)
plot(1:4, Recovery.Knee.y(4:7,1), 'x', 'LineWidth', 1.5)
hold on
plot(1:4, Recovery.Knee.y(4:7,2), '*', 'LineWidth', 1.5)
hold on
plot(1:4, Recovery.Knee.y(4:7,3), 'o', 'LineWidth', 1.5)
errorbar(Recovery.Knee.y(4:7,2), Recovery.Knee.err(4:7), 'r', 'LineStyle',
'none', 'LineWidth', 1.5)
title('Maximum Butterfly Recovery Knee Internal Rotation Vs. ROM')
legend('Active ROM', 'Butterfly Max', 'Passive ROM')
xlim([0 5])
xticks([1 2 3 4])
```

```
xticklabels([Recovery.Knee.x{4}; Recovery.Knee.x{5}; Recovery.Knee.x{6};
Recovery.Knee.x{7}])
ylabel('Joint Angle [deg]')

subplot(3,1,3)
plot(1:2, Recovery.Knee.y(8:9,1), 'x', 'LineWidth', 1.5)
hold on
plot(1:2, Recovery.Knee.y(8:9,2), '*', 'LineWidth', 1.5)
hold on
plot(1:2, Recovery.Knee.y(8:9,3), 'o', 'LineWidth', 1.5)
errorbar(Recovery.Knee.y(8:9,2), Recovery.Knee.err(8:9), 'r', 'LineStyle',
'none', 'LineWidth', 1.5)
title('Maximum Butterfly Recovery Knee Flexion Vs. ROM')
legend('Active ROM', 'Butterfly Max', 'Passive ROM')
xlim([0 3])
xticks([1 2])
xticklabels([Recovery.Knee.x{8}; Recovery.Knee.x{9}])
ylabel('Joint Angle [deg]')

%% Create Function to Eliminate Outliers and Calculate Average Without Outliers
function [output] = PRO(xx)

%% Organize Data into Drop and Recovery Max
xx.Min = - xx.Min; % Make all joint angle positive
JA = [xx.Max, xx.Min]; % Combined data from all joint motion into one single
matrix
JA = nonzeros(JA); % Remove all 0 values
JA = reshape(JA, 30, length(JA)/30); % Reshape matrix

%% Eliminate Outliers
for i = 1:min(size(JA))
    ave(i) = mean(JA(:,i)); % Average joint angles from single motion
    stand_dev(i) = std(JA(:,i)); % Find standard deviation of joint angles from
single motion
    thresh_high(i) = ave(i) + 2 * stand_dev(i); % Use ave + 2std as upper
threshold
    thresh_low(i) = ave(i) - 2 * stand_dev(i); % Use ave - 2std as lower
threshold

    for j = 1 length(JA);
        if JA(j,i) >= thresh_high(i)
            JA(j,i) = 0; % Remove outliers over the upper limit
        else if JA(j,i) <= thresh_low(i)
                JA(j,i) = 0; % Remove outliers lower than the lower limit
            else
                JA(j,i) = JA(j,i); % Keep the rest of the data within range
            end
        end
    end
end

%% Find Average Max
for i = 1:min(size(JA))
    ave(i) = mean(nonzeros(JA(:,i))); % Find new average after outliers are
removed
    stand_dev(i) = std(nonzeros(JA(:,i))); % Find new standard deviation after
outliers are removed
end

%% Output Results
output.ave = ave;
output.stand_dev = stand_dev;
```

```
end

%% Create Function to Process ROM Data
function [output] = ROM(xx);
rom = [xx.Max, xx.Min]; % Put all ROM into a single matrix

%% Separate Drop and Recovery
Drop = [rom(1:7), rom(9:16), rom(24), rom(27), rom(29), rom(31)]; % ROM needed
for dropping motion
Recovery = [rom(1:16), rom(18), rom(24), rom(26:27), rom(29), rom(31)]; % ROM
needed for recovery motion

%% Take out Knee Rotations and Ab/Adduction
for i = 1: length(Drop)
    if Drop(i) == 0;
        Drop(i) = NaN;
    else
        Drop(i) = Drop(i);
    end
end

for i = 1: length(Recovery)
    if Recovery(i) == 0;
        Recovery(i) = NaN;
    else
        Recovery(i) = Recovery(i);
    end
end

%% Output Results
output.Drop = Drop;
output.Recovery = Recovery;

end

%% Create Function to Group Data for Graphing
function [output] = Group(xx, yy, zz);

for i = 1:length(xx.ave)
    y(i,1) = yy(i); % Active ROM
    y(i,2) = xx.ave(i); % Average during butterfly
    y(i,3) = zz(i); % Passive ROM

    stand_dev(i) = xx.stand_dev(i); % Errors during butterfly

end

%% Output Results
output.y = y;
output.err = stand_dev;

end
```

C. MATLAB Script for Raw Force Plate Data Processing

```
%% Thesis Force Plate
%% Tzu-Ting (Tiffany) Hsu
clear all
close all
clc

%% Loading Force Plate Data
filename = input('Type in file name');
RCut = input('Row number of the last force plate data minus 1');
CCut = input('Column number of the last force plate data minus 1');
FP = csvread(filename, 5, 2, [5, 2, RCut, CCut]);

%% Seperate Data of Each Force Plate and Camera
FP1 = FP(:, 19:27);
FP2 = FP(:, 1:9); % Big FP
FP3 = FP(:, 10:18);
% FP_C = FP(:, 28:36);

%% Downsampling Force Plate Data
FP1 = resample(FP1, 3, 50);
FP2 = resample(FP2, 3, 50);
FP3 = resample(FP3, 3, 50);
% FP_C = resample(FP_C, 3, 50);

%% Export to Ascii
dlmwrite('FP_BF_NoSkate03_walking02.txt',FP2, 'delimiter', '\t', 'precision',
6);
```

D. MATLAB for Inverse Dynamic Data Processing

```
%% Thesis Inverse Dynamic
% Tzu-Ting (Tiffany) Hsu
clear all
close all
clc

%% Loading Force Plate Data - Butterfly 1
BF1.JRF_H = dlmread('FP_BF1_R_Hip_JRF.txt', '\t', 2, 2);
BF1.JRM_H = dlmread('FP_BF1_R_Hip_JRM.txt', '\t', 2, 2);
BF1.JRF_K = dlmread('FP_BF1_R_Knee_JRF.txt', '\t', 2, 2);
BF1.JRM_K = dlmread('FP_BF1_R_Knee_JRM.txt', '\t', 2, 2);
BF1.FP = dlmread('FP_BF_Skate_Tr04.txt', '\t');

%% Loading Force Plate Data - Butterfly 2
BF2.JRF_H = dlmread('FP_BF2_R_Hip_JRF.txt', '\t', 2, 2);
BF2.JRM_H = dlmread('FP_BF2_R_Hip_JRM.txt', '\t', 2, 2);
BF2.JRF_K = dlmread('FP_BF2_R_Knee_JRF.txt', '\t', 2, 2);
BF2.JRM_K = dlmread('FP_BF2_R_Knee_JRM.txt', '\t', 2, 2);
BF2.FP = dlmread('FP_BF_Skate_Tr05.txt', '\t');

%% Loading Force Plate Data - Butterfly 3
BF3.JRF_H = dlmread('FP_BF3_R_Hip_JRF.txt', '\t', 2, 2);
BF3.JRM_H = dlmread('FP_BF3_R_Hip_JRM.txt', '\t', 2, 2);
BF3.JRF_K = dlmread('FP_BF3_R_Knee_JRF.txt', '\t', 2, 2);
BF3.JRM_K = dlmread('FP_BF3_R_Knee_JRM.txt', '\t', 2, 2);
BF3.FP = dlmread('FP_BF_Skate_Tr06.txt', '\t');

%% Loading Force Plate Data - Butterfly 4
BF4.JRF_H = dlmread('FP_BF4_R_Hip_JRF.txt', '\t', 2, 2);
BF4.JRM_H = dlmread('FP_BF4_R_Hip_JRM.txt', '\t', 2, 2);
BF4.JRF_K = dlmread('FP_BF4_R_Knee_JRF.txt', '\t', 2, 2);
BF4.JRM_K = dlmread('FP_BF4_R_Knee_JRM.txt', '\t', 2, 2);
BF4.FP = dlmread('FP_BF_Skate_Tr07.txt', '\t');

%% Loading Force Plate Data - Butterfly 5
BF5.JRF_H = dlmread('FP_BF5_R_Hip_JRF.txt', '\t', 2, 2);
BF5.JRM_H = dlmread('FP_BF5_R_Hip_JRM.txt', '\t', 2, 2);
BF5.JRF_K = dlmread('FP_BF5_R_Knee_JRF.txt', '\t', 2, 2);
BF5.JRM_K = dlmread('FP_BF5_R_Knee_JRM.txt', '\t', 2, 2);
BF5.FP = dlmread('FP_BF_Skate_Tr08.txt', '\t');

%% Loading Force Plate Data - Squating
SS.JRF_H = dlmread('FP_Squating_R_Hip_JRF.txt', '\t', 2, 2);
SS.JRM_H = dlmread('FP_Squating_R_Hip_JRM.txt', '\t', 2, 2);
SS.JRF_K = dlmread('FP_Squating_R_Knee_JRF.txt', '\t', 2, 2);
SS.JRM_K = dlmread('FP_Squating_R_Knee_JRM.txt', '\t', 2, 2);
SS.FP = dlmread('FP_BF_NoSkate03_Squat01.txt', '\t');

%% Loading Force Plate Data - Walking
Gait.JRF_H = dlmread('FP_Walking_R_Hip_JRF.txt', '\t', 2, 2);
Gait.JRM_H = dlmread('FP_Walking_R_Hip_JRM.txt', '\t', 2, 2);
Gait.JRF_K = dlmread('FP_Walking_R_Knee_JRF.txt', '\t', 2, 2);
Gait.JRM_K = dlmread('FP_Walking_R_Knee_JRM.txt', '\t', 2, 2);
Gait.FP = dlmread('FP_BF_NoSkate03_Walking01.txt', '\t');

%% Find the Impact Point for Butterfly Data
[pks, IP1] = min(BF1.FP(:,3));
[pks, IP2] = min(BF2.FP(:,3));
[pks, IP3] = min(BF3.FP(:,3));
[pks, IP4] = min(BF4.FP(:,3));
```

```
[pks, IP5] = min(BF5.FP(:,3));

%% Find Maximum for the Butterfly Drop
BF1.Max = [max(BF1.JRF_H(1:(IP1-1),:)); max(BF1.JRM_H(1:(IP1-1),:)); ...
    max(BF1.JRF_K(1:(IP1-1),:)); max(BF1.JRM_K(1:(IP1-1),:))];
BF2.Max = [max(BF2.JRF_H(1:(IP2-1),:)); max(BF2.JRM_H(1:(IP2-1),:)); ...
    max(BF2.JRF_K(1:(IP2-1),:)); max(BF2.JRM_K(1:(IP2-1),:))];
BF3.Max = [max(BF3.JRF_H(1:(IP3-1),:)); max(BF3.JRM_H(1:(IP3-1),:)); ...
    max(BF3.JRF_K(1:(IP3-1),:)); max(BF3.JRM_K(1:(IP3-1),:))];
BF4.Max = [max(BF4.JRF_H(1:(IP4-1),:)); max(BF4.JRM_H(1:(IP4-1),:)); ...
    max(BF4.JRF_K(1:(IP4-1),:)); max(BF4.JRM_K(1:(IP4-1),:))];
BF5.Max = [max(BF5.JRF_H(1:(IP5-1),:)); max(BF5.JRM_H(1:(IP5-1),:)); ...
    max(BF5.JRF_K(1:(IP5-1),:)); max(BF5.JRM_K(1:(IP5-1),:))];

BF1.Min = [min(BF1.JRF_H(1:(IP1-1),:)); min(BF1.JRM_H(1:(IP1-1),:)); ...
    min(BF1.JRF_K(1:(IP1-1),:)); min(BF1.JRM_K(1:(IP1-1),:))];
BF2.Min = [min(BF2.JRF_H(1:(IP2-1),:)); min(BF2.JRM_H(1:(IP2-1),:)); ...
    min(BF2.JRF_K(1:(IP2-1),:)); min(BF2.JRM_K(1:(IP2-1),:))];
BF3.Min = [min(BF3.JRF_H(1:(IP3-1),:)); min(BF3.JRM_H(1:(IP3-1),:)); ...
    min(BF3.JRF_K(1:(IP3-1),:)); min(BF3.JRM_K(1:(IP3-1),:))];
BF4.Min = [min(BF4.JRF_H(1:(IP4-1),:)); min(BF4.JRM_H(1:(IP4-1),:)); ...
    min(BF4.JRF_K(1:(IP4-1),:)); min(BF4.JRM_K(1:(IP4-1),:))];
BF5.Min = [min(BF5.JRF_H(1:(IP5-1),:)); min(BF5.JRM_H(1:(IP5-1),:)); ...
    min(BF5.JRF_K(1:(IP5-1),:)); min(BF5.JRM_K(1:(IP5-1),:))];

% Averaging Maximum for the Butterfly Drop
for i = 1:4
    for j = 1:3
        BF_Max(i,j) = mean([BF1.Max(i,j), BF2.Max(i,j), BF3.Max(i,j),
BF4.Max(i,j), BF5.Max(i,j)]);
        BF_Min(i,j) = mean([BF1.Min(i,j), BF2.Min(i,j), BF3.Min(i,j),
BF4.Min(i,j), BF5.Min(i,j)]);
    end
end

% Finding the maximum load for the right direction for butterfly
for i = 1:4
    for j = 1:3
        if abs(BF_Max(i,j)) < abs(BF_Min(i,j))
            Final.BF(i,j) = BF_Min(i,j);
        else
            Final.BF(i,j) = BF_Max(i,j);
        end
    end
end

%% Find Maximum for Single Leg Squats
[pks, start] = findpeaks(SS.FP(:,3), 'MinPeakHeight', -400, 'MinPeakWidth', 5);
SS.Max = zeros(4,3,5);
for i = 1:5
    SS.Max(:,:,i) = [max(SS.JRF_H(start(2*i-1):start(2*i),:));
max(SS.JRM_H(start(2*i-1):start(2*i),:)); ...
        max(SS.JRF_K(start(2*i-1):start(2*i),:)); max(SS.JRM_K(start(2*i-
1):start(2*i),:))];
    SS.Min(:,:,i) = [min(SS.JRF_H(start(2*i-1):start(2*i),:));
min(SS.JRM_H(start(2*i-1):start(2*i),:)); ...
        min(SS.JRF_K(start(2*i-1):start(2*i),:)); min(SS.JRM_K(start(2*i-
1):start(2*i),:))];
end

% Averaging Maximum for the Single Leg Squats
for i = 1:4
```

```
    for j = 1:3
        SS_Max (i,j) = mean(SS.Max(i,j,:));
        SS_Min (i,j) = mean(SS.Min(i,j,:));
    end
end

% Finding the maximum load for the right direction for single leg squat
for i = 1:4
    for j = 1:3
        if abs(SS_Max(i,j)) < abs(SS_Min(i,j))
            Final.SS(i,j) = SS_Min(i,j);
        else
            Final.SS(i,j) = SS_Max(i,j);
        end
    end
end

%% Find Maximum for Walking
Gait.Max = [max(Gait.JRF_H(:,:)); max(Gait.JRM_H(:,:)); ...
    max(Gait.JRF_K(:,:)); max(Gait.JRM_K(:,:))];
Gait.Min = [min(Gait.JRF_H(:,:)); min(Gait.JRM_H(:,:)); ...
    min(Gait.JRF_K(:,:)); min(Gait.JRM_K(:,:))];

%% Finding the maximum load for the right direction
for i = 1:4
    for j = 1:3
        if abs(BF_Max(i,j)) < abs(BF_Min(i,j))
            Final.BF(i,j) = BF_Min(i,j);
        else
            Final.BF(i,j) = BF_Max(i,j);
        end

        if abs(SS_Max(i,j)) < abs(SS_Min(i,j))
            Final.SS(i,j) = SS_Min(i,j);
        else
            Final.SS(i,j) = SS_Max(i,j);
        end

        if abs(Gait.Max(i,j)) < abs(Gait.Min(i,j))
            Final.Gait(i,j) = Gait.Min(i,j);
        else
            Final.Gait(i,j) = Gait.Max(i,j);
        end
    end
end
```

E. Results for Medial Vs. Lateral Lower Leg Sensor Placement Test

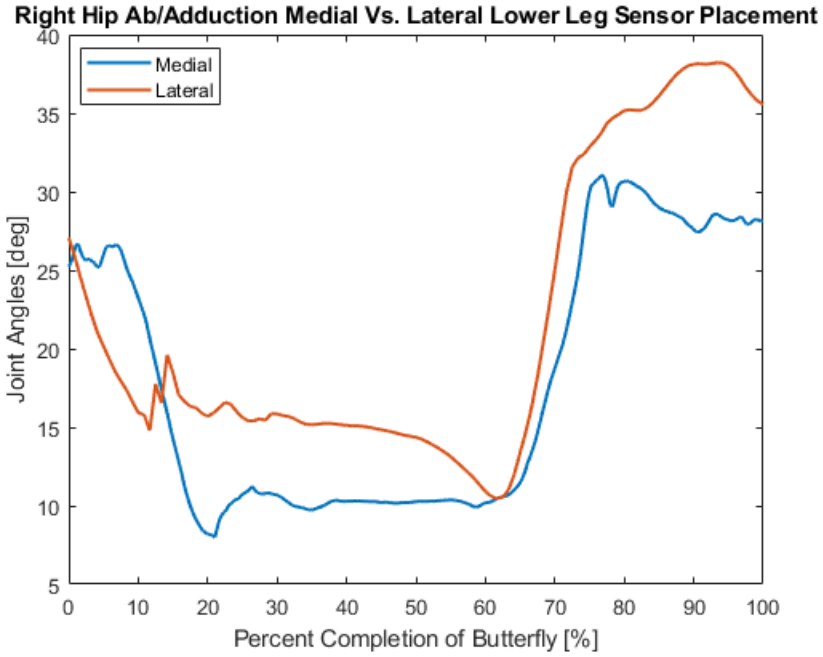

Figure 30. Right hip abduction/adduction joint angle of a single butterfly with lower leg sensors placing on the medial side and the lateral side of the leg. Positive direction is abduction and negative is adduction.

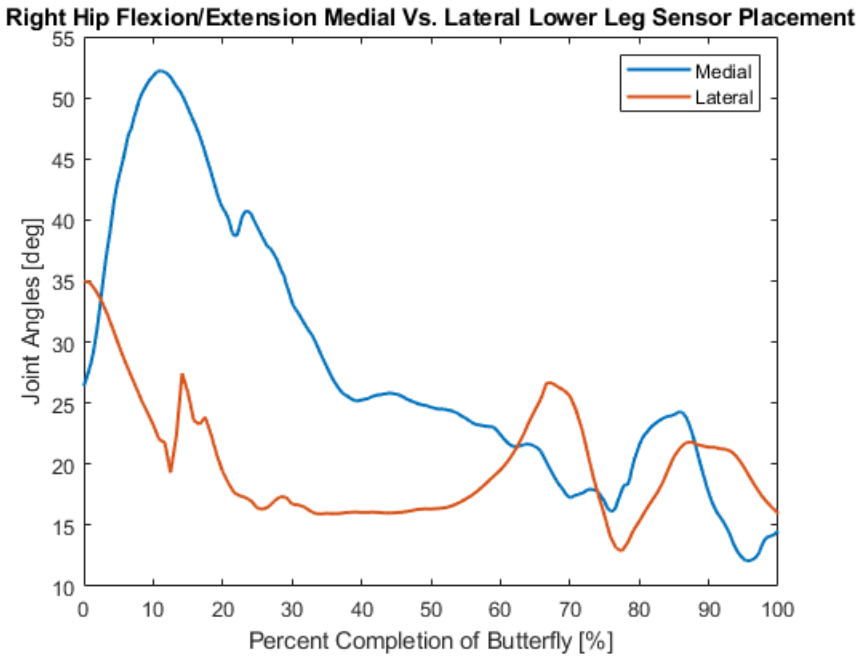

Figure 31. Right hip flexion/extension joint angle of a single butterfly with lower leg sensors placing on the medial side and the lateral side of the leg. Positive direction is flexion and negative is extension.

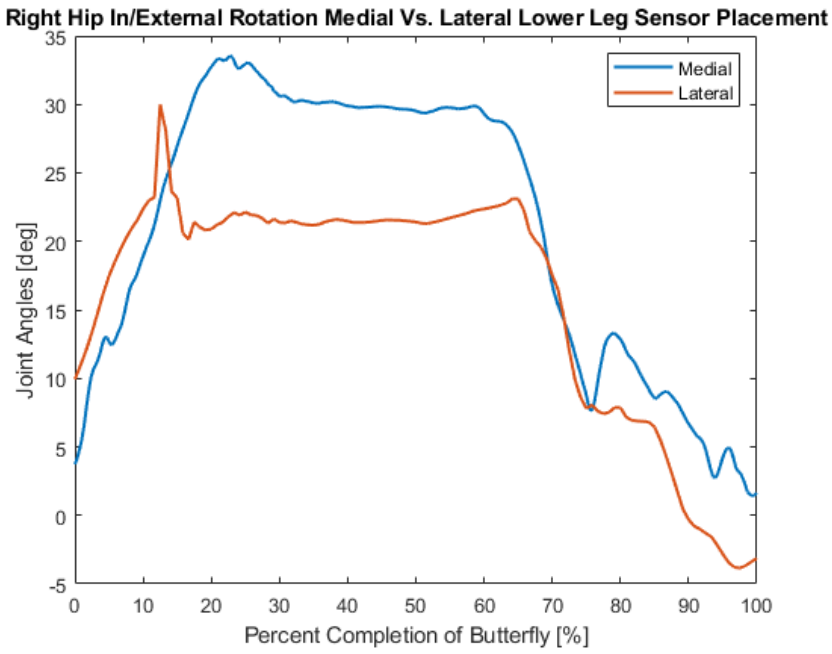

Figure 32. Right hip internal/external rotation joint angle of a single butterfly with lower leg sensors placing on the medial side and the lateral side of the leg. Positive direction is internal rotation and negative is external rotation.

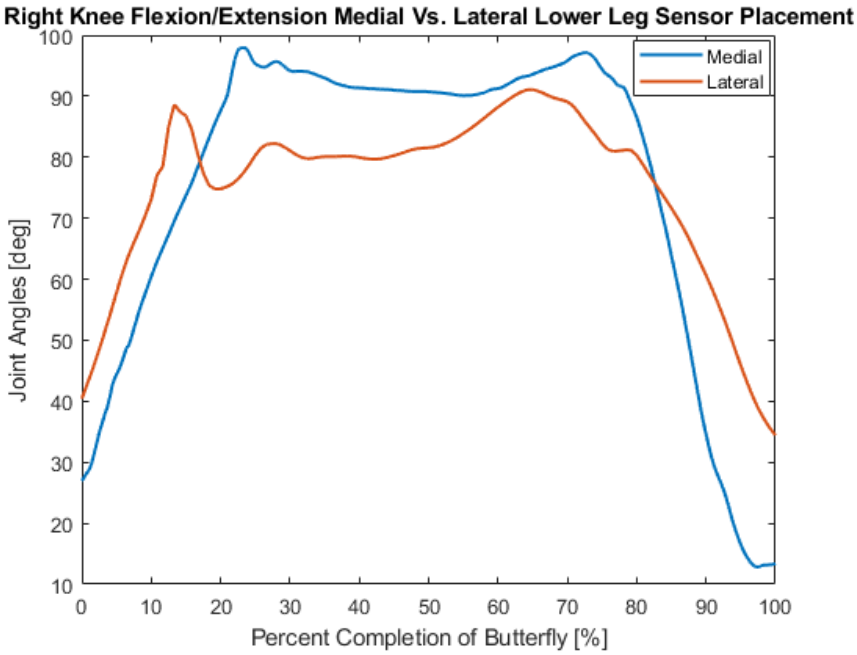

Figure 33. Right knee flexion/extension joint angle of a single butterfly with lower leg sensors placing on the medial side and the lateral side of the leg. Positive direction is flexion and negative is extension.

F. Results for Repeatability Test

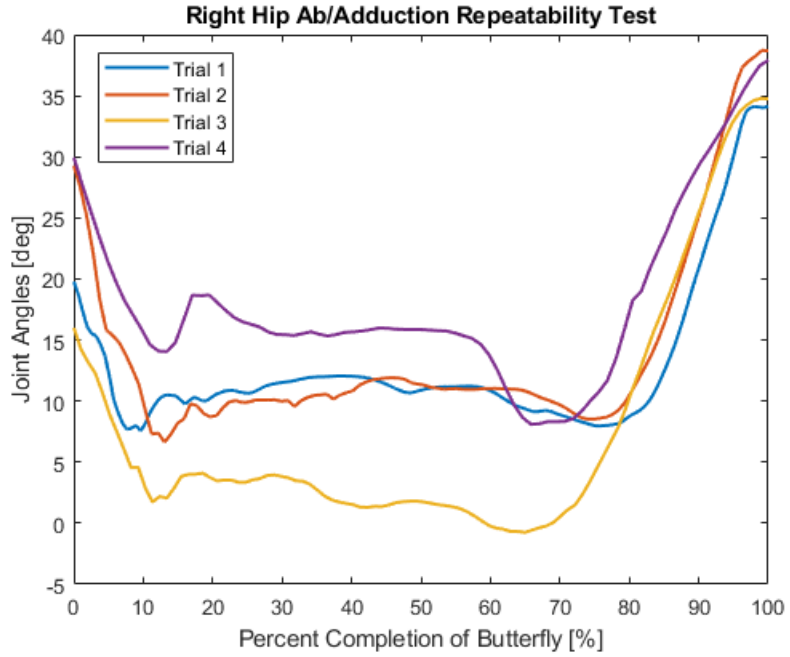

Figure 34. Right hip abduction/adduction of one butterfly with four different trials. Trial 1 and 2 are from the same capture and 3 and 4 are from the same capture. Positive direction is abduction and negative is adduction.

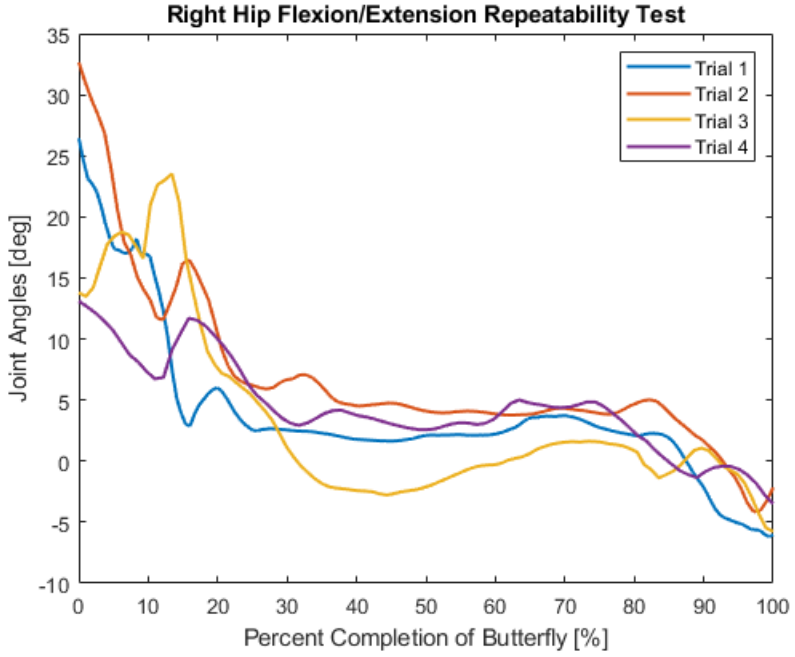

Figure 35. Right hip flexion/extension rotation of one butterfly with four different trials. Trial 1 and 2 are from the same capture and 3 and 4 are from the same capture. Positive direction is flexion and negative is extension.

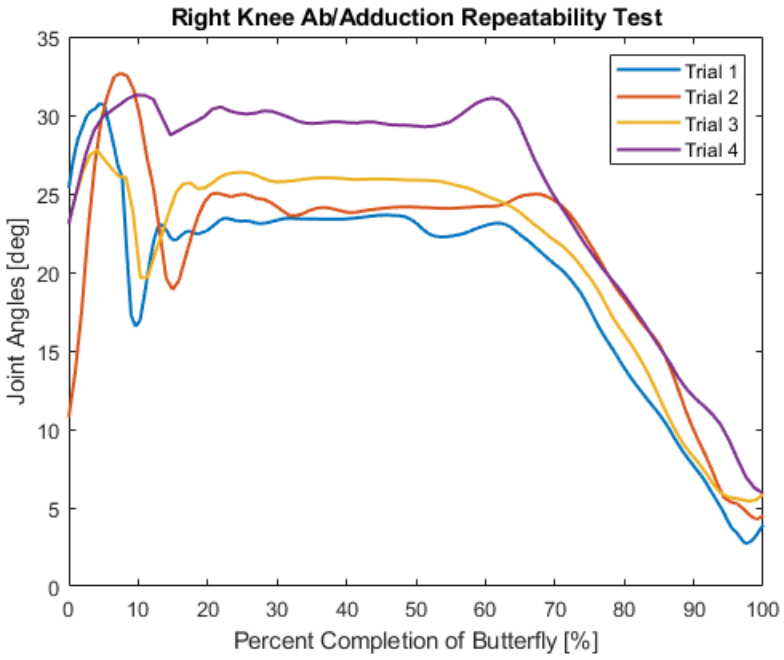

Figure 36. Right knee abduction/adduction of one butterfly with four different trials. Trial 1 and 2 are from the same capture and 3 and 4 are from the same capture. Positive direction is abduction and negative is adduction.

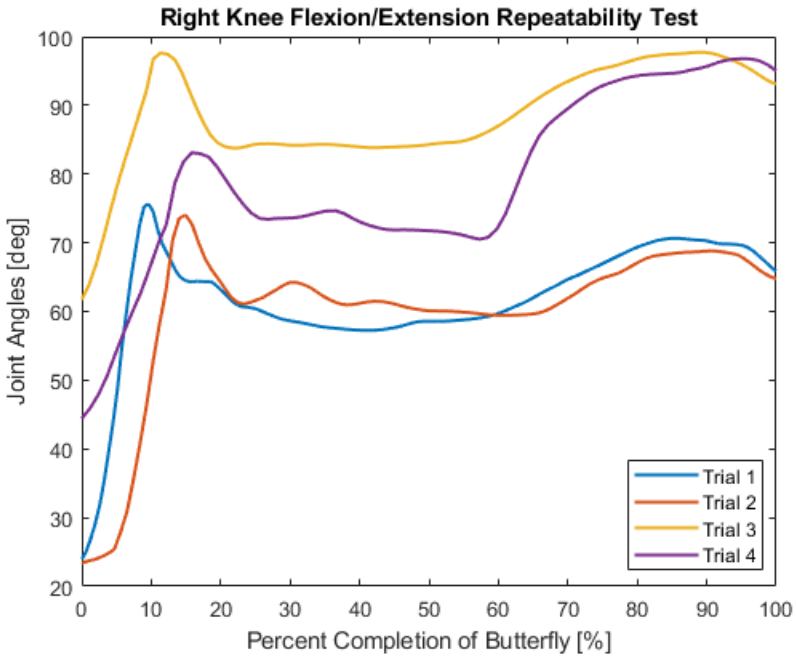

Figure 37. Right knee flexion/extension of one butterfly with four different trials. Trial 1 and 2 are from the same capture and 3 and 4 are from the same capture. Positive direction is flexion and negative is extension.

G. Joint Angle for 1 Butterfly

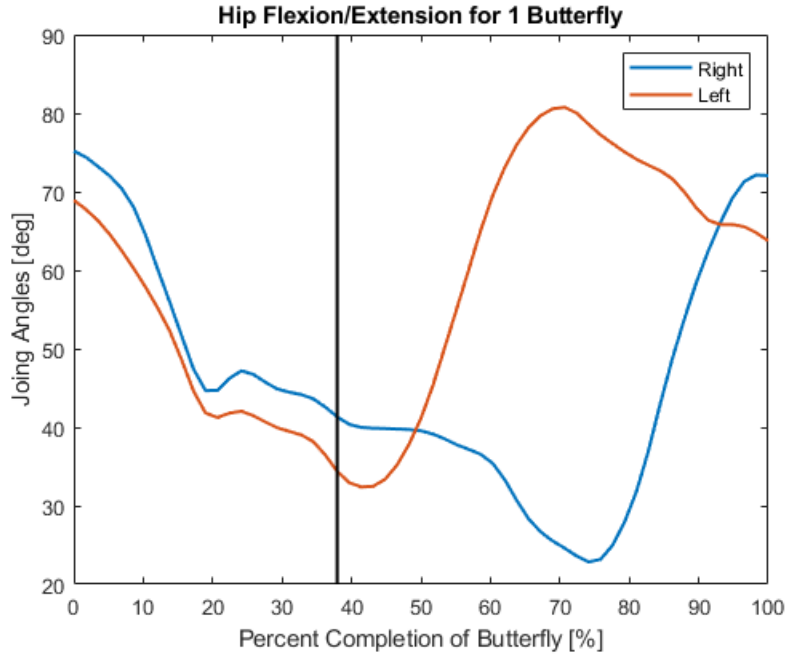

Figure 38. Hip flexion/extension joint angle for one butterfly. The black line going vertically indicates the start of the recovery process. Positive direction is flexion and negative is extension.

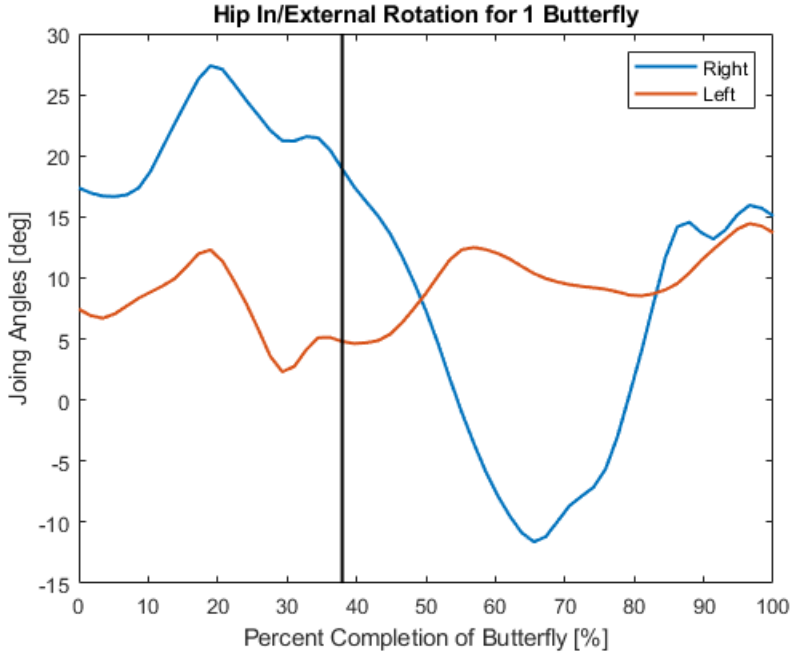

Figure 39. Hip internal/external rotation joint angle for one butterfly. The black line going vertically indicates the start of the recovery process. Positive direction is internal rotation and negative is external rotation.

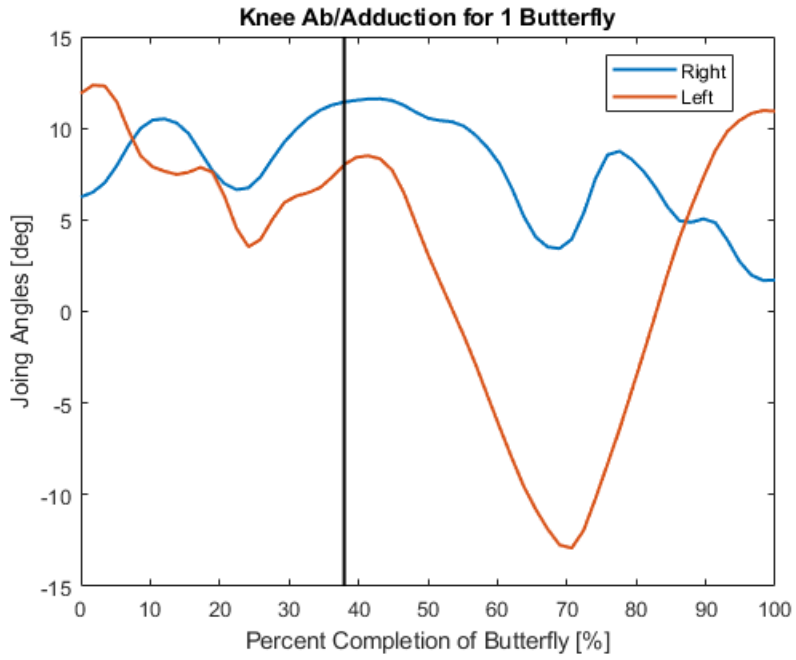

Figure 40. Knee abduction/adduction joint angle for one butterfly. The black line going vertically indicates the start of the recovery process. Positive direction is abduction and negative is adduction.

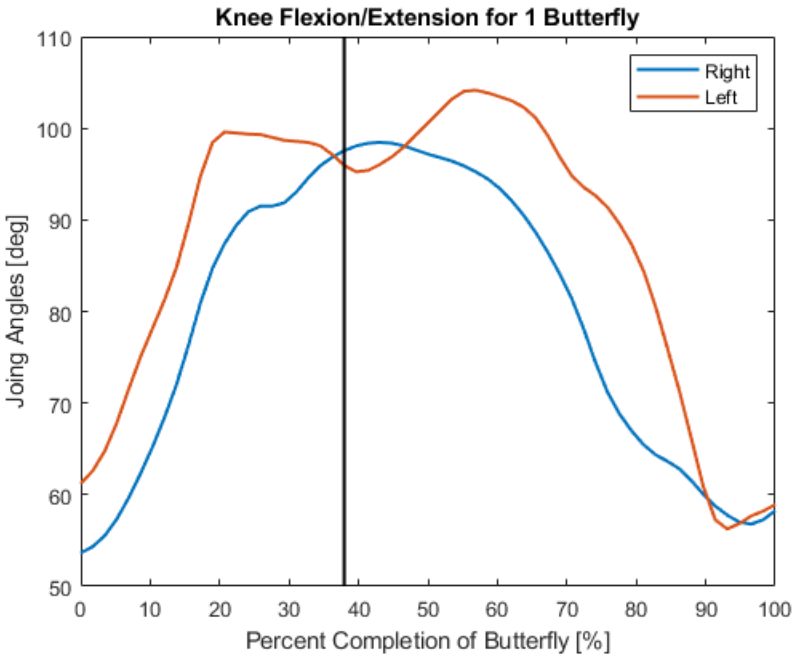

Figure 41. Knee flexion/extension joint angle for one butterfly. The black line going vertically indicates the start of the recovery process. Positive direction is flexion and negative is extension.

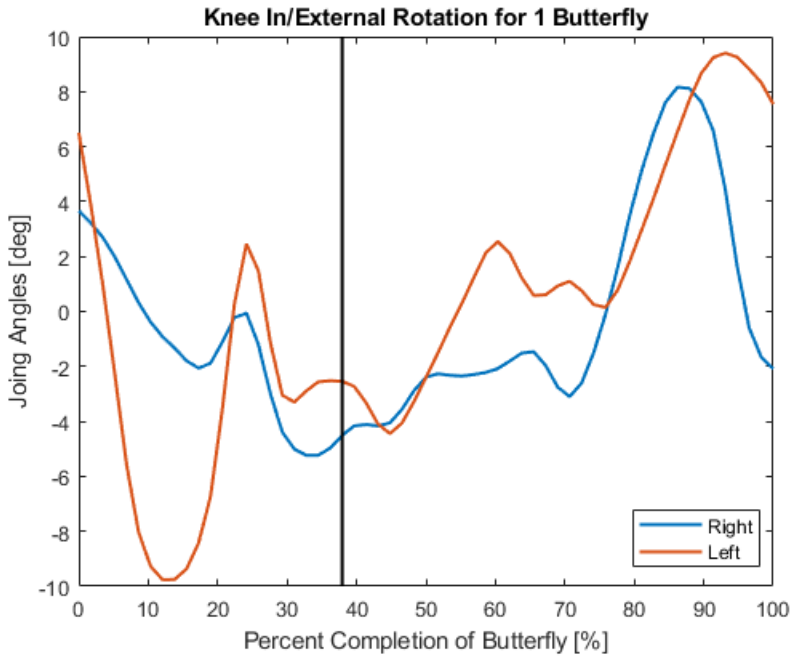

Figure 42. Knee internal/external rotation joint angle for one butterfly. The black line going vertically indicates the start of the recovery process. Positive direction is internal rotation and negative is external rotation.

H. Plots for Random Uncertainties

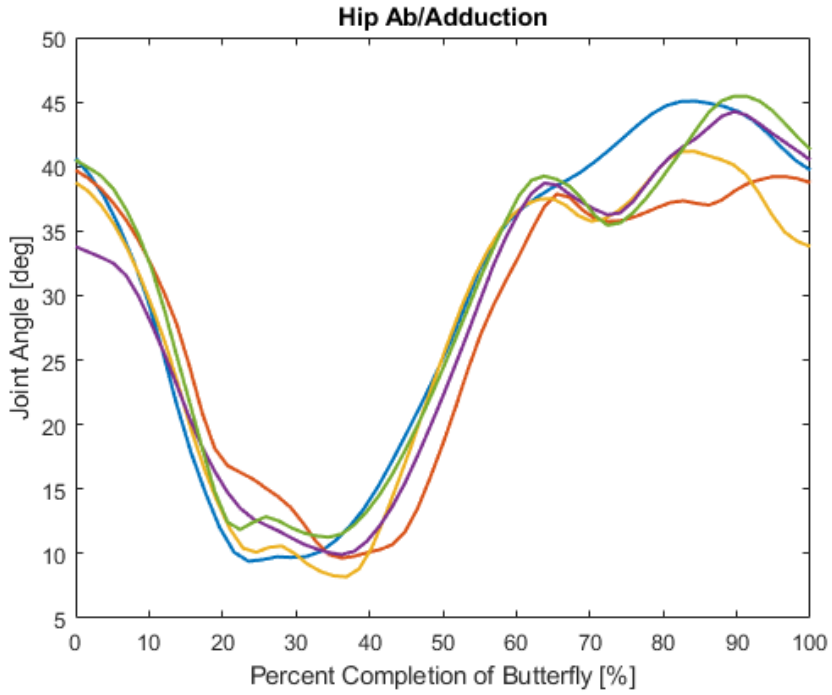

Figure 43. 5 trials of right hip abduction/adduction angles during butterfly motion. Positive direction is abduction and negative is adduction.

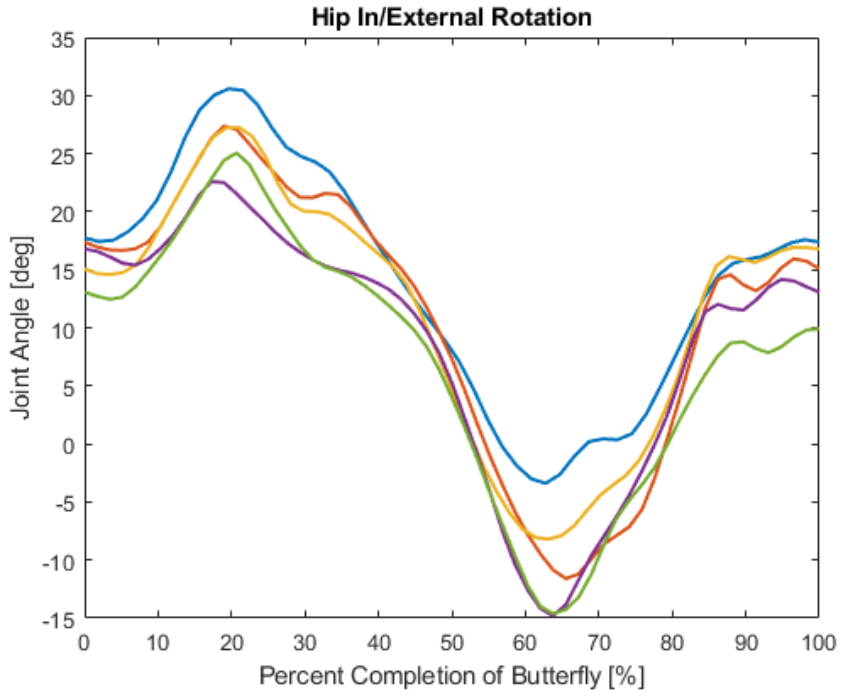

Figure 44. 5 trials of right hip internal/external rotation angles during butterfly motion. Positive direction is internal rotation and negative is external rotation.

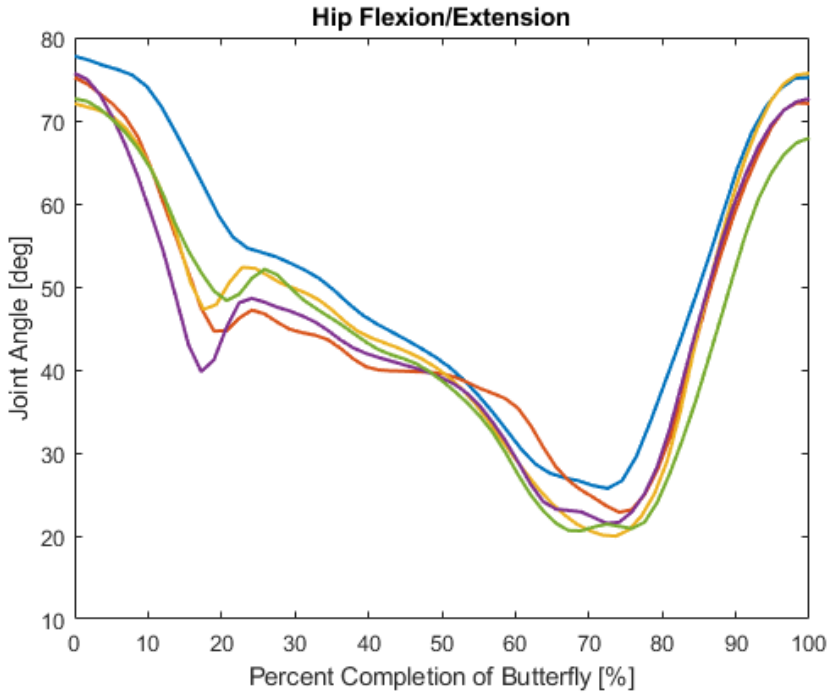

Figure 45. 5 trials of right hip flexion/extension angles during butterfly motion. Positive direction is flexion and negative is extension.

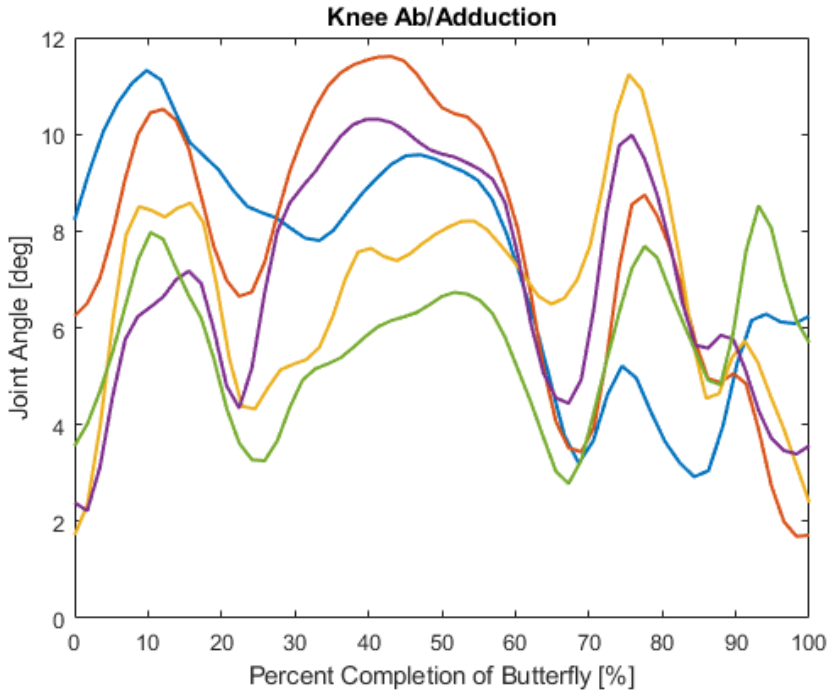

Figure 46. 5 trials of right knee abduction/adduction angles during butterfly motion. Positive direction is abduction and negative is adduction.

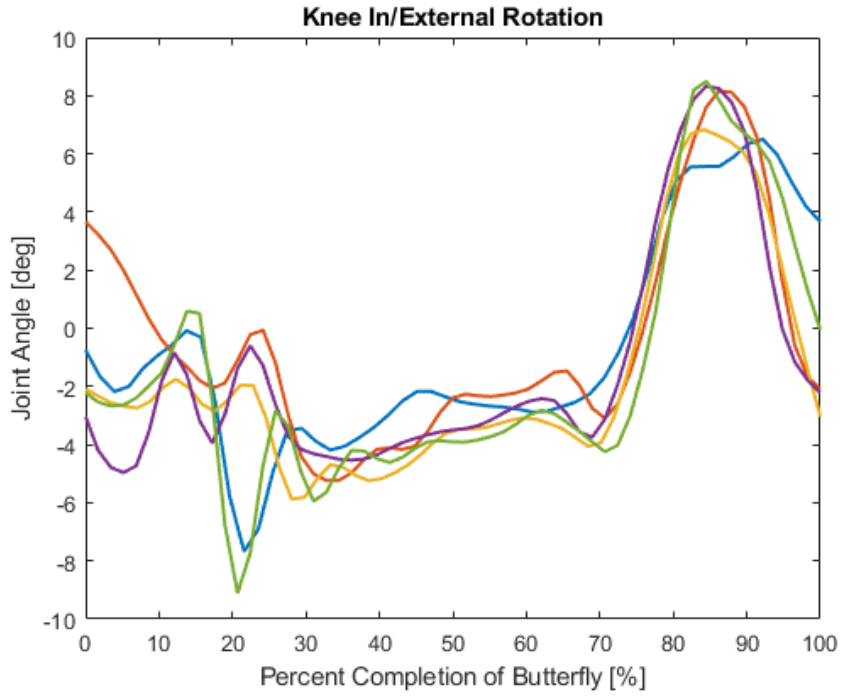

Figure 47. 5 trials of right knee internal/external rotation angles during butterfly motion. Positive direction is internal rotation and negative is external rotation.

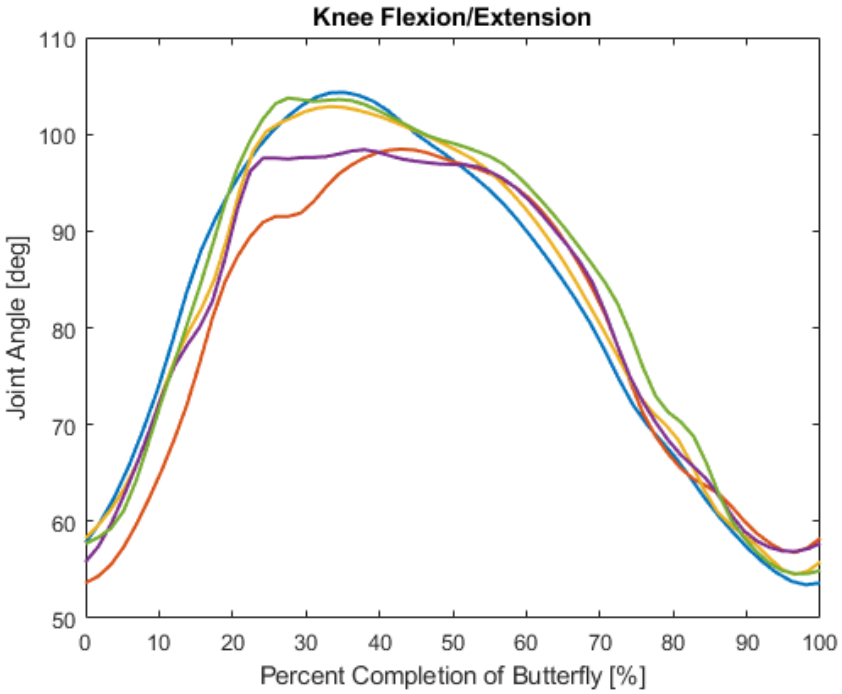

Figure 48. 5 trials of right knee flexion/extension angles during butterfly motion. Positive direction is flexion and negative is extension.

I. Xsens MVNX Awinda Spec Sheet

Xsens MVN (Hardware)

MVN Link			MVN Awinda
	Lycra suit	**Version**	Strap-based 
	17 wired trackers	**Trackers**	17 wireless trackers
	Validated & proven	**Data**	Validated & proven
	Fast	**Setup**	Even faster
	20 ms	**Latency**	30 ms
	One Access Point for multiple persons	**Data link**	One Awinda station per person
	One battery	**Battery management**	17 batteries
	10 hours	**Battery life**	6 hours
		Wireless range:	
	50 m / 150 ft	**In the lab**	20 m / 60 ft
	150 m / 450 ft	**Outdoor**	50 m / 150 ft
	Yes	**On-body recording**	No
	10 min	**On-body buffering**	2 min
	1000 Hz	**Internal sampling rate**	1000 Hz
	240 Hz	**Output rate**	60 Hz (Full body) 100 HZ (Lower body)
	Natively supports Manus VR Glove	**Finger tracking**	Natively supports Manus VR Glove

MVN Analyze (Software)

Feature	MVN Analyze
Multi Person	Yes
Network Streamer (for plug-ins)	Yes, all major analysis packages
Advanced Configurations	Yes
Advanced Scenarios	Yes
Reference Camera support	Yes
Export as movie	Yes
Time code & remote control	Yes
Batch export	No
Analyze Engine	
Real-time solver	Yes
HD Reprocessor	Yes

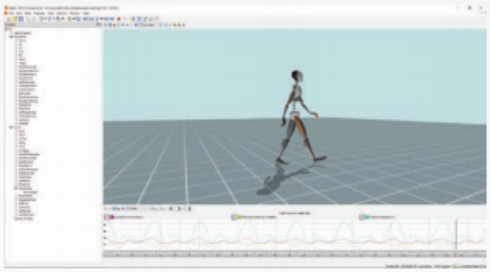

J. AMTI Force Plates Spec Sheet

AMTI
FORCE AND MOTION

www.AMTI.biz | sales@amtimail.com

OR6-6-OP-1000 SPECIFICATIONS

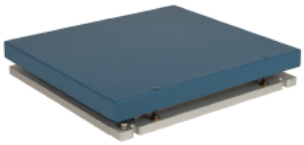

AMTI's OR6-6-OP is an industry "standard size" force plate for gait studies and is used in hundreds of labs around the world. High sensitivity, low crosstalk, excellent repeatability and long-term stability make this platform an ideal candidate for research and clinical studies. It also features a low-mass composite top plate that provides excellent frequency response, perfect for analysis of athletic performance, running and jumping.

The OR6-6-OP features AMTI's advanced Optima technology – providing industry leading accuracy at no additional cost.

Key performance features include:

- Average COP accuracy of just a fraction of a millimeter (typically less than 0.4 mm)
- Crosstalk values typically ±0.2% of applied load
- Measurement accuracy typically ±0.25% of applied calibration load*

Units: Metric ▼ Capacity: 4448 N ▼

Dimensions(WxLxH)	464 x 508 x 82.55 mm	**Mounting hardware**	Recommended
Weight	18.18 Kg.	**Sensing elements**	Strain gage bridge
Channels	Fx, Fy, Fz, Mx, My, Mz	**Amplifier**	Required included OPT-SC
Top plate material	Composite	**Analog outputs**	6 Channels
Temperature range	-17.78 to 51.67°C	**Digital outputs**	USB: see Notes below
Excitation	10V maximum	**Crosstalk***	± 0.20% on all channels
Fx, Fy, Fz hysteresis	±0.2% full scale output		
COP Accuracy*	± 0.4 mm.	**Measurement Accuracy***	± 0.25% of applied load

*Typical value: minimum applied load of 222.4 N (50 lb.)

AMTI
FORCE AND MOTION

www.AMTI.biz | sales@amtimail.com

Channel	**Fx**	**Fy**	**Fz**	**Units**	**Mx**	**My**	**Mz**	**Units**
Capacity	2224	2224	4448	N	1129	1129	565	N-m
Sensitivity	0.674	0.674	0.169	µv/v-N	1.59	1.59	3.37	µv/v-N-m
Natural frequency	400	400	1000	Hz	-	-	-	Hz

Notes: Digital output is achieved with the included **Optima Signal Conditioner**

Published specifications subject to change without notice.

Last modified:2017-11-28

TECHNICAL DRAWING

Footprint Drawing

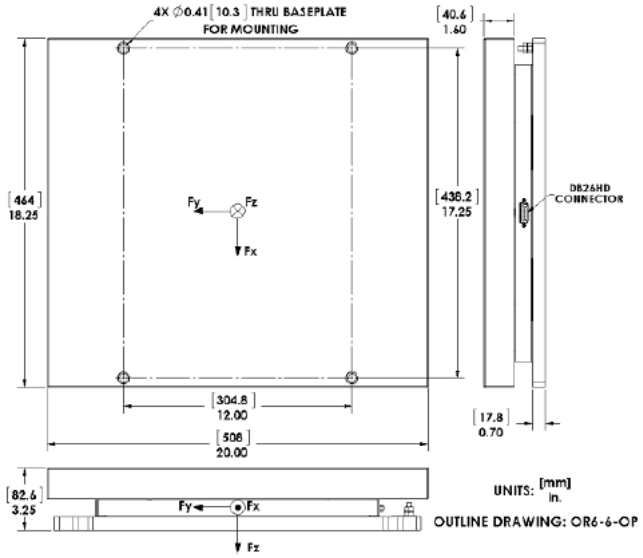

Electrical Drawing

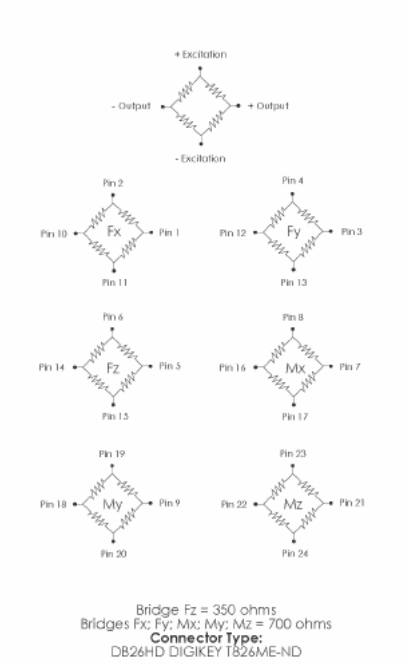

Bridge Fz = 350 ohms
Bridges Fx; Fy; Mx; My; Mz = 700 ohms
Connector Type:
DB26HD DIGIKEY T826ME-ND

AMTI FORCE AND MOTION www.AMTI.biz | sales@amtimail.com

BP600900-1000 SPECIFICATIONS

The BP900900 offers a large target area, perfect for sports performance analysis.

Sorry, no image is currently available.

Units: Metric ▼ Capacity: 4448 N ▼

Dimensions(WxLxH)	600 x 900 x 101.6 mm	**Mounting hardware**	Recommended
Weight	31.82 Kg.	**Sensing elements**	Strain gage bridge
Channels	Fx, Fy, Fz, Mx, My, Mz	**Amplifier**	Required - see Notes below
Top plate material	Composite	**Analog outputs**	6 Channels
Temperature range	-17.78 to 51.67°C	**Digital outputs**	USB: see Notes below
Excitation	10V maximum	**Crosstalk**	< 2% on all channels
Fx, Fy, Fz hysteresis	± 0.2% full scale output	**Fx, Fy, Fz non-linearity**	± 0.2% full scale output

AMTI FORCE AND MOTION www.AMTI.biz | sales@amtimail.com

Channel	Fx	Fy	Fz	Units	Mx	My	Mz	Units
Capacity	2224	2224	4448	N	203	1355	1016	N-m
Sensitivity	0.674	0.674	0.169	µv/v-N	0.93	1.03	2.06	µv/v-N-m
Natural frequency	270	270	500	Hz	-	-	-	Hz

Notes:

Higher capacities available, please consult AMTI

Digital output is achievable with the **Gen 5 Amplifier**

Published specifications subject to change without notice.

Last modified:2017-11-28

TECHNICAL DRAWING

Footprint Drawing

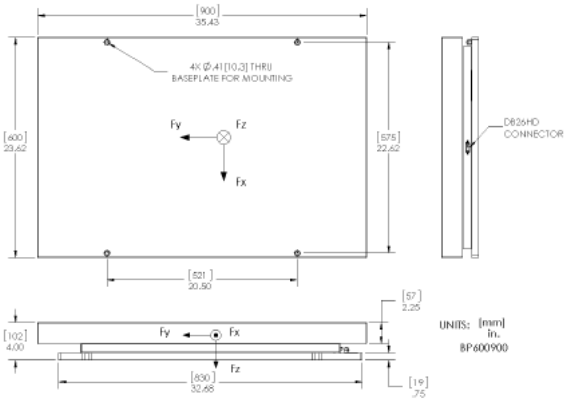

Electrical Drawing

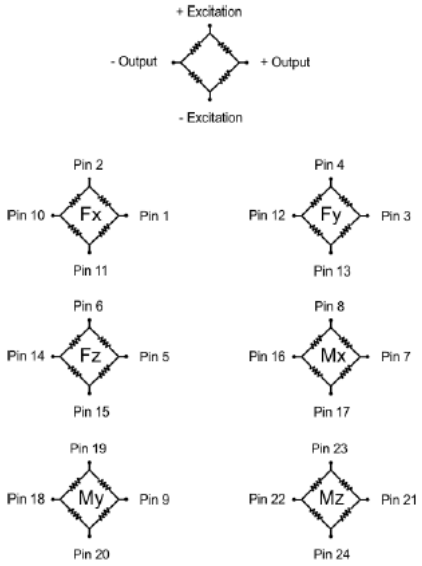

Bridges Fz = 350 Ohms
Bridges Fx; Fy; Mx; My; Mz = 700 Ohms

Connector Type:

DR26HD DIGIKEY T826MF-ND

K. IRB Human Subject Approval

R·I·T

Rochester Institute of Technology

RIT Institutional Review Board for the
Protection of Human Subjects in Research
141 Lomb Memorial Drive
Rochester, New York 14623-5604
Phone: 585-475-7673
Fax: 585-475-7990
Email: hmfsrs@rit.edu

Form C
IRB Decision Form
FWA# 00000731

TO: Kathleen Lamkin-Kennard

FROM: RIT Institutional Review Board

DATE: **December 4, 2018**

RE: **Decision of the RIT Institutional Review Board**

Project Title – Acquisition of Hockey Goalies Kinematic data with Inertial Motion Capture Systems

The Institutional Review Board (IRB) has taken the following action on your project named above:

☒ Approved, no greater than minimal risk

Now that your project is approved, you may proceed as you described in the Form A. **Note that this approval is only for a maximum of 12 months; you may conduct research on human subjects only between the date of this letter and December 4, 2018.**

You are required to submit to the IRB any:

- **Proposed** modifications and wait for approval before implementing them,
- Unanticipated risks, and
- Actual injury to human subjects.

Return the Form F, at the end of your human research project or 12 months from the above date. If your project will extend more than 12 months, your project must receive continuing review by the IRB.

Continuing review of research and approval of research studies is required so long as the research study is ongoing, that is, until research-related interactions and interventions with human subjects or the obtaining and analysis of identifiable private information described in the IRB-approved research plan have been completed.

Investigators are responsible for submitting sufficient materials and information for the IRB to meet its regulatory obligations, and should follow the institutional policies and procedures for continuing IRB review of research that are required by HHS regulations at (45 CFR 46.103(b)(4), 45 CFR 46.109(e), 45 CFR 46.115(a)(1)) as appropriate to the research activity.

Heather Foti, MPH
Associate Director
Human Subjects Research Office

Revised 08.17.2017